Acta Mech. Sin. (2015) 31(4):425–445
DOI 10.1007/s10409-015-0464-z

REVIEW PAPER

Molecular tagging techniques and their applications to the study of complex thermal flow phenomena

Fang Chen[1,2] · **Haixing Li**[1] · **Hui Hu**[1]

Received: 28 October 2014 / Revised: 10 February 2015 / Accepted: 27 April 2015 / Published online: 4 August 2015

Abstract This review article reports the recent progress in the development of a new group of *molecule-based* flow diagnostic techniques, which include molecular tagging velocimetry (MTV) and molecular tagging thermometry (MTT), for both qualitative flow visualization of thermally induced flow structures and quantitative whole-field measurements of flow velocity and temperature distributions. The MTV and MTT techniques can also be easily combined to result in a so-called molecular tagging velocimetry and thermometry (MTV&T) technique, which is capble of achieving simultaneous measurements of flow velocity and temperature distribution in fluid flows. Instead of using tiny particles, the molecular tagging techniques (MTV, MTT, and MTV&T) use phosphorescent molecules, which can be turned into long-lasting glowing marks upon excitation by photons of appropriate wavelength, as the tracers for the flow velocity and temperature measurements. The unique attraction and implementation of the molecular tagging techniques are demonstrated by three application examples, which include: (1) to quantify the unsteady heat transfer process from a heated cylinder to the surrounding fluid flow in order to examine the thermal effects on the wake instabilities behind the heated cylinder operating in mixed and forced heat convection regimes, (2) to reveal the time evolution of unsteady heat transfer and phase changing process inside micro-sized, icing water droplets in order to elucidate the underlying physics pertinent to aircraft icing phenomena, and (3) to achieve simultaneous droplet size, velocity and temperature measurements of "in-flight" droplets to characterize the dynamic and thermodynamic behaviors of flying droplets in spray flows.

Keywords Molecular tagging velocimetry · Molecular tagging thermometry · Wake instabilities behind the heated cylinder · Aircraft icing · Icing physics of water droplets · Dynamics and thermodynamics of flying droplets in spray flows

1 Introduction

The behavior of fluid flows influences and often determines the performance of a large variety of functional devices and processes. Some of the more familiar examples include fuel/air mixing in internal combustion (IC) engines and combustors, and aerodynamics of air flows around airborne vehicles like airplanes and helicopters. To understand and control the behavior of fluid flows, quantitative information is needed on velocity, temperature, and density/concentration or pressure at many points simultaneously (i.e., quantitative whole-field maps of multiple flow variables). Of these variables, velocity and temperature are considered to be among the most important.

Presently, whole-field velocity measurements in turbulent flows are commonly performed with *particle-based* diagnostic techniques like particle image velocimetry (PIV) [1] and global Doppler velocimetry (GDV) [2,3], or planar Doppler velocimetry (PDV) [4,5]. These techniques rely on seeding the flow with particles and observing the motion of the tracer particles to derive fluid velocity. A sheet of laser light is usually used to illuminate the region of interest. The tracer particles scatter the laser light as they move through it. In PIV,

✉ Hui Hu
huhui@iastate.edu

[1] Department of Aerospace Engineering, Iowa State University, Ames, IA 50011, USA

[2] School of Aeronautics & Astronautics, Shanghai Jiao Tong University, Shanghai 200240, China

photographic film or charge-coupled device (CCD) detectors are used to record the positions of the tracer particles. The positions are recorded at two different times, separated by a prescribed time interval. The displacements of individual particles, or more often groups of particles, are determined by well-developed computer-intensive procedures. The displacements over the known time interval provide the estimate of the particle velocity vectors. In GDV or PDV, the scattering from the tracer particles is imaged through a molecular filter whose transmission is proportional to the wavelength of the light. The particles are illuminated with a very narrow line-width laser, and the frequency shift associated with the particle velocity leads to a change in the particle brightness as seen through the filter. When compared to a reference image, a velocity map of the tracer particles can be realized. For particle-based velcoimetry techniques, the velocity vectors of the working fluid are deduced based on the assumption that the tracer particles move with the same velocities as the working fluids.

Since the *particle-based* velocimetry techniques measure the velocity vectors of *tracer particles*, not the velocity vectors of *working fluid* directly, several issues or implications may arise from the fact that they do not directly measure fluid motion but, rather infer it from the motion of tracer particles. For example, to apply the *particle-based* velocimetry techniques for thermal flow studies, the effects of the inertia and buoyancy forces acting on the tracer particles must be carefully considered in order to make a physically meaningful measurement of fluid velocity. The *particle-based* measurements may actually become "intrusive" when the size of tracer particles is comparable with that of the measurement domain for microfluidics and micro-scale heat transfer studies. The applications of *particle-based* flow measurement techniques can also be hampered by the potential interaction of tracer particles with walls [6,7] or by complications arising from the electrothermal, electrophoretic, and dielectrophorectic forces that act on tracer particles but do not originate from working fluids [8,9]. For example, when microscopic PIV (i.e., μPIV) technique is applied to study electroosmotic flows (EOFs), the derived velocity is actually the sum of the electrophoretic velocity of the charged tracer particles and the electroosmotic velocity of the bulk neutral fluid [9]. It is usually quite difficult and troublesome, if not impossible, to precisely decouple the electrophoretic velocity and the electroosmotic velocity, especially for cases with significant temperature variations in EOFs due to Joule heating [10]. The implications of using *particle-based* flow diagnostic techniques would become much more complicated for heat transfer studies, where the density of working fluid (e.g., air or water) usually changes with temperature while the density of tracer particles usually does not.

Using molecules, instead of tiny particles, as the tracers for flow measurements is expected to significantly mitigate, and perhaps even eliminate, these implications and/or issues. Even for the cases where the issues related to the ability of tracer particles to follow the flow motion are negligible, there are still many situations in which the presence of tracer particles is undesirable—they may interfere with the operation of a device (for example, in confined flows, the tracer particles may coat the windows leading to limited test times or even window abrasion) or change flow physics completely due to the existence of the tracer particles (for example, as described in Ref. [11], in an icing physics study to examine the transient phase changing process of liquid water turning into solid ice, tracer particles in the water would serve as the starting sites to initial the solidification process, which changes the icing physics completely). In such cases, *molecule-based* approaches can offer significant advantages over the *particle-based* flow diagnostic techniques.

Planar laser-induced fluorescence (LIF) technique has been widely used to conduct temperature measurements in fluid flows. For some fluorescent molecules, such as acetone [12,13] and Rhodamine B [14,15], the absorption coefficient and quantum efficiency are usually temperature dependent. Therefore, in principle, fluorescence intensity may be considered to depend only on temperature as long as the incident laser excitation is uniform and the concentration of the tracer molecules remains constant in the measurement region. However, in practice, it can be difficult to ensure a temporally and spatially non-varying incident laser excitation and uniform molecular tracer concentration in the measurement region for some applications. This may cause significant errors in the temperature measurement results.

In order to eliminate the effects of the non-uniformity of molecular tracer concentration and the spatially non-varying incident laser excitation on the temperature measurement, several *ratiometric* LIF techniques, which included the two-dye approach [14,16], the single-dye, two-emission-band method [17], and the dual-excitation-wavelength approach [18], have been developed recently. For these *ratiometric* LIF techniques, two cameras with various optical filters are usually required, along with a very careful image registration or coordinate mapping procedure in order to get the quantitative spatial relation between the two acquired fluorescence images. In addition, other complications also need to be carefully considered, such as the spectral conflicts and photobleaching behavior of the two fluorescent dyes in the two-dye approach [16]. In the single-dye, two-emission-band method, the LIF signal reduction caused by the integration of emission over a narrow spectral band necessitates special attention to issues such as low signal-to-noise ratio and the choices of the image recording system and optical filters [17]. The dual-excitation-wavelength LIF technique [18] requires two different lasers to excite fluorescence tracer molecules at two different wavelengths, which may complicate the exper-

imental setup and add extra burdens on the instrumentation cost for the measurements.

Since fluorescence emission usually has a very short lifetime, which is on the order of nanoseconds, *LIF-based* thermometry techniques usually rely on the information obtained from the *"intensity axis"* of the photoluminescence emission process [10,19]. The fluorescence images are usually acquired while the laser excitation is still illuminating the flow, leading to potential contamination of the LIF signal by the reflection and/or scattering of the incident laser light. The use of optical filters to mitigate this problem may result in a reduction of the LIF signal because the Stokes shift (i.e., shift in wavelength towards red) between the absorption and fluorescence emission spectra is usually small. Depending on the extent of the Stokes shift, it is sometimes very difficult to eliminate such contaminations completely.

Laser-induced phosphorescence (LIP) techniques have also been suggested recently to conduct temperature measurements for thermal flow studies [20–22]. Compared with *LIF-based* thermometry techniques, the Stokes shift in *LIP* is typically much larger. Therefore, it is much easier to filter out the artifacts caused by the excitation source for *LIP-based* measurements. Furthermore, LIP was also found to be much more sensitive to temperature variation compared with LIF [19,20], which is favorable for the accurate measurements of small temperature differences in the thermal flow studies. The molecular tagging thermometry (MTT) technique to be introduced in the present study is actually a *LIP-based thermometry* technique.

In the present study, the recent progress in the development of a new group of *molecule-based* flow diagnostic techniques, which include molecular tagging velocimetry (MTV) [23–25] and MTT [10,22,26], for both qualitative flow visualization of thermally induced flow structures and quantitative whole-field measurements of flow velocity and temperature distributions, will be reported. Essentially, the MTV technique is the *molecular* counterpart of the PIV technique for the flow velocity measurements. The MTV and MTT techniques can be easily combined to result in a so-called molecular tagging velocimetry and thermometry (MTV&T) technique [26,27], which is capable of achieving simultaneous measurements of flow velocity and temperature distribution in fluid flows. Instead of using tiny particles, the molecular tagging techniques (MTV, MTT, and MTV&T) use phosphorescent molecules, which can be turned into long-lasting glowing marks upon excitation by photons of appropriate wavelength, as the tracers for the flow velocity and temperature measurements. A pulsed laser is typically used to "tag" the tracer molecules in the regions of interest, and the tagged molecules are imaged at two successive times within the photoluminescence lifetime of the tracer molecules. The measured Lagrangian displacement of the tagged molecules provides the estimate of the fluid velocity. The simultaneous temperature measurement is achieved by taking advantage of the temperature dependence of phosphorescence lifetime, which is estimated from the intensity ratio of the tagged molecules in the acquired two phosphorescence images

As completely *molecule-based* approaches, the molecular tagging techniques can greatly mitigate, if not eliminate, the issues or implications constricting the application of *particle-based* flow diagnostic techniques in thermal flow studies. Furthermore, it can provide simultaneous measurements of multiple flow quantities such as temperature and velocity distributions in fluid flows, instead of measuring flow velocity vectors only, which *particle-based* techniques like PIV, GDV, or PDV can barely, if not at all, provide as the measurement results.

In the sections that follow, the technical basis of the molecular tagging techniques is described briefly along with the related properties of the molecular tracers commonly used for flow velocity and/or temperature measurements. The unique attraction of the molecular tagging techniques will be demonstrated from three application examples that use the molecular tagging techniques to study complex thermal flow phenomena, which include: (1) to quantify the unsteady heat transfer process from a heated cylinder to the surrounding fluid flow in order to examine the thermal effects on the wake instabilities behind the heated cylinder operating in mixed and forced heat convection regimes, (2) to reveal the time evolution of unsteady heat transfer and phase changing process inside small icing water droplets in order to elucidate the underlying physics pertinent to the ice formation and accretion processes as water droplets impinge onto frozen cold aircraft wings, and (3) to achieve simultaneous droplet size, velocity, and temperature measurements of "in-flight" droplets to characterize the dynamic and thermodynamic behaviors of flying droplets in spray flows pertinent to the atomization and evaporation processes of the fuel droplets in combustion chambers of gas turbine engines.

2 Technical basis of the molecular tagging techniques

2.1 Commonly-used molecular tracers for quantitative measurements in fluid flows

2.1.1 Molecular tracers for flow diagnostics in gaseous flows

The most commonly used molecular tracers for quantitative flow velocity and/or temperature measurements in gaseous flows are Biacetyl [28] and Acetone [29]. Biacetyl

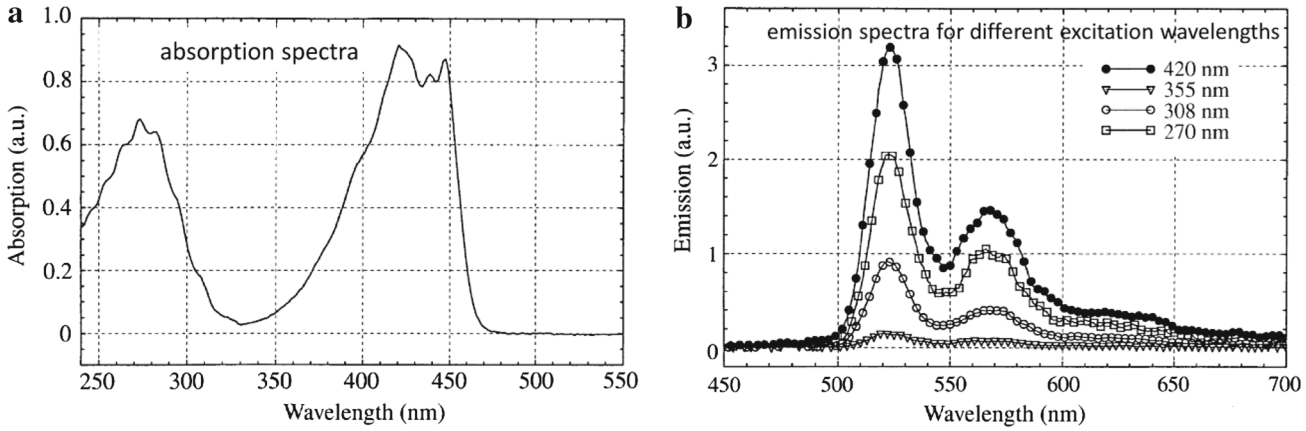

Fig. 1 The absorption and emission spectrum of Biacetyl [25]

($CH_3COCOCH_3$, also called 2,3-Butanedione) has been used extensively for flow visualization and quantitative flow velocity, temperature, and density measurements. Due to its relatively high vapor pressure (i.e., on the order of millibars at room temperature), Biacetyl is readily seeded into gaseous flows allowing a molar seeding fraction of about 5 %. Figure 1 shows the absorption and emission spectrum of Biacetyl, which is taken from Stier and Koocheshahani [25]. As shown in Fig. 1a, Biacetyl has quite strong absorption within a wide wavelength range with two strong absorption peaks centered at 270 and 430 nm. It suggests that most of the commonly used UV lasers in the lab, such as quadrupled Nd:YAG lasers with an excitation wavelength of 266 nm or XeCl-filled excimer lasers at the wavelength of 308 nm, can be suitable as the excitation source for the flow measurements with Biacetyl as the molecular tracer. Upon the pulsed laser excitation at a proper wavelength, the phosphorescence lifetime of Biacetyl can be as long as 1.5 ms in an oxygen-free flow. However, the phosphorescence lifetime of Biacetyl was found to be reduced dramatically in air flows due to a strong oxygen quenching effect [25]. It should also be noted that, although Biacetyl, which is actually used as a food additive, is considered as non-toxic, it can exude a pungent smell so as to need some additional care for the experiments with Biacetyl as the molecular tracer. Further information about the chemical and photoluminescence properties of Biacetyl is available in Refs. [25,28].

Acetone is another most commonly used molecular tracer for quantitative flow velocity and/or temperature measurements in gaseous flows [29,30]. In comparison to Biacetyl, Acetone has a higher vapor pressure, and is somewhat easier to work with. While the photoluminescence properties of Acetone is quite similar to those of Biacetyl, Acetone has a very strong absorption within the wavelength range of 230–340 nm, which is well matched to the excitation wavelength of quadrupled Nd:YAG lasers (i.e., fourth harmonic at 266 nm) or XeCl lasers (i.e., excitation wavelength at 308 nm).

Several other molecular tracers have also been used for flow velocity and/or temperature measurements in gaseous flows. For example, Miles and his team [31,32] used vibrationally excited O_2 as the molecular tracer to examine supersonic mixing of helium and air in association with fuel–air mixing in hypersonic engines. Also, Pitz and his group [33,34] used OH (dissociation of H_2O) as the molecular tracer to achieve flow velocity measurement in air flows and a flame. Other molecular tracers used for quantitative flow measurements in gaseous flows also include nitrogen dioxide [35], tert-butyl nitrite [36,37], sodium [38], and strontium [39]. Further information about the promising molecular tracers for quantitative flow measurements in gaseous flows can be found in the references [23,34,40].

2.1.2 Molecular tracers used for MTV and/or MTT measurements in liquid-phase flows

While a large number of fluorescent dyes or molecular tracers have been used for qualitative flow visualization and quantitative flow temperature and concentration measurements in liquid phase flows, the chemical and photoluminescence properties of the most commonly used fluorescent dyes can be found in the review article of Coppta and Rogers [16]. The focus of the present study is on the molecular tracers which have been used for MTV and/or MTT measurements in liquid-phase flows.

Since the early work of Miller [41], photochromic molecules have been widely used for visualizing flow and flow velocity measurements in liquid flows [42,43]. For example, a laser- induced photochemical anemometry (LIPA) technique, which is considered as an earlier version of MTV technique, was developed by using photochromic molecules as the molecular tracer to achieve flow velocity measurements in liquid flows [44,45]. Caged fluorescein dye was also

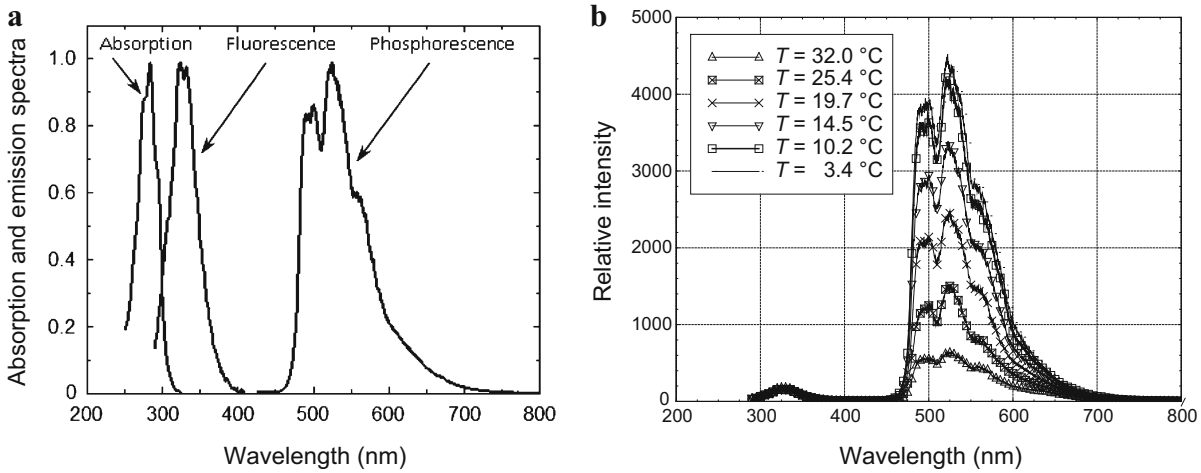

Fig. 2 Absorption and emission spectra of 1-BrNp · Gβ-CD · ROH triplex [19]. **a** Normalized absorption and emission spectra. **b** Emission spectra at different temperatures

used to conduct flow measurements within a free falling water droplet [46]. More recently, a specially-designed, water-soluble phosphorescent supramolecules 1-BrNp · Gβ-CD · ROH triplex [47,48], has been extensively used as the molecular tracer for MTV and MTT measurements in liquid flows. The phosphorescent triplex is actually a mixture of a compound of three different chemicals, which are lumophore (indicated collectively by 1-BrNp), glucosyl-β-cyclodextrin (indicated collectively by Gβ-CD), and alcohols (indicated collectively by ROH).

It has been found that, both the emission intensity and lifetime of photoluminescence of the 1-BrNp · Gβ-CD · ROH triplex would vary substantially as the concentrations of each chemical compound of the triplex changes. As originally suggested by Gendrich et al. [47], a concentration of 2×10^{-4} M for Mβ-CD, a saturated (approximately 1×10^{-5} M) solution of 1-BrNp, and a concentration of 0.06 M for the alcohol (ROH) are the most commonly used settings for MTV and/or MTT measurements in recent years. Further information about the chemical and photoluminescence properties of the 1-BrNp · Gβ-CD · ROH triplex is available at Refs. [23,24,48].

Figure 2 shows the absorption and emission spectrum of the 1-BrNp · Mβ-CD · ROH triplex. It can be clearly seen that the absorption range of 1-BrNp · Mβ-CD · ROH molecules is quite narrow with the absorption peak near 280 nm. The absorption coefficients of the triplex would become almost zero as the excitation wavelength is greater than 325 nm. Consequently, Excimer lasers with the excitation wavelength of 308 nm or quadrupled Nd:YAG lasers at the excitation wavelength of 266 nm are usually used to excite 1-BrNp · Mβ-CD · ROH molecules for flow velocity and temperature measurements. It can also be seen that, upon the laser excitation at proper wavelengths, the 1-BrNp · Mβ-CD · ROH triplex would emit both fluorescence and phosphorescence. The phosphorescence emission is significantly red shifted relative to fluorescence, as expected. Because of the large red shift, there is no overlap between the phosphorescence emission and absorption spectra, and the phosphorescence does not get reabsorbed. It should be noted that, Pouya et al. [49] recently demonstrated the feasibility of using multi-photon excitation by ultrafast femtosecond lasers at the wavelength of 400 nm to effectively excite the 1-BrNp · Mβ-CD · ROH triplex for MTV measurements in an aqueous flow. It suggests that, nonlinear multi-photon excitation holds great promise for elimination of the need for a short wavelength UV excitation source and UV optical access in flow facilities for molecular tagging measurements.

As shown clearly in Fig. 2b, the phosphorescence emission of the 1-BrNp · Mβ-CD · ROH triplex is very temperature sensitive, while its fluorescence emission intensity is almost independent of the temperature. While the fluorescence lifetime of the 1-BrNp · Mβ-CD · ROH triplex is very short, i.e., within 20 ns, the phosphorescence lifetime was found to be much longer, which is on the order of milliseconds [27]. It was also found that the phosphorescence lifetime of the 1-BrNp · Mβ-CD · ROH triplex would vary significantly as the fluid temperature changes [11,22,26]. Figure 3 gives the measured phosphorescence lifetimes of the 1-BrNp · Mβ-CD · ROH triplex as a function of temperature [11]. It can be seen clearly that, the phosphorescence lifetime of the 1-BrNp · Mβ-CD · ROH triplex was found to decrease from about 7.2 ms to 0.4 ms as the temperature varies from 1.0 °C to 50.0 °C. The relative temperature sensitivity of the phosphorescence lifetime varies from about 5.0 % per °C at 20 °C to 20.0 % per °C at 50 °C, which is much higher than those of the most commonly used fluorescent dyes. For comparison, the temperature sensitivity of Rhodamine B, i.e., the most commonly used dye in LIF-based thermometry, is only about 2.0 % per °C [19]. The enhanced temperature sensi-

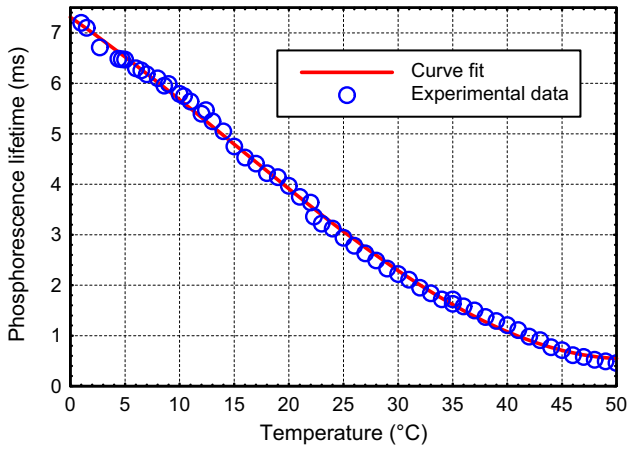

Fig. 3 Phosphorescence lifetime of 1-BrNp · Mβ-CD · ROH triplex versus temperature [11]

tivity of the LIF-based thermometry reported by Shafii et al. [50], which utilizes a two-color, two-dye, approach with two temperature sensitive fluorescent dyes of opposite temperature sensitivities, has been to be about 4.0 % per °C.

It should also be noted, for most commonly used fluorescent dyes, their fluorescence intensities are usually pH sensitive[16]. As reported in Hu et al. [10], while the total intensities of both fluorescence and phosphorescence emissions of the phosphorescent triplex 1-BrNp · Mβ-CD · ROH molecules were found to be pH sensitive, their phosphorescence lifetime is almost independent of the pH value of the solution (i.e., variations within 1.0 %). It suggests that, the 1-BrNp · Mβ-CD · ROH triplex can be used as a very promising molecular tracer in various analytical chemistry and biological studies involving both pH and temperature variations in the applications.

2.2 Molecular tagging velocimetry techniques

Several *molecule-based* flow diagnostic techniques have been developed in recent years for achieving whole-field velocity measurements in fluid flows. They can be categorized as "Doppler-shift" methods and "time-of-flight" methods.

With "Doppler-shift" methods, flow velocity is deduced from the small Doppler shift of the wavelength of the Rayleigh scattering light [51,52] or LIF signal of some special molecule tracers [13,53]. These methods are the *molecular* counterparts of the GDV or PDV technique. They are more accurate at higher velocities because the Doppler shift is larger and, therefore, more easily measured. However, they often only yield averaged flow velocities due to a lack of signal strength. Also with the Doppler-shift methods, the optical geometry of the excitation laser and observer define the velocity component that is measured, which can be limiting for some applications [4,54,55].

The "time-of-flight" methods are also called MTV or flow tagging velocimetry techniques [25,28,32,33,35,47], which are recently reviewed by Koochesfahani and Nocera [23]. These methods are the *molecular* counterpart of the PIV technique. The special molecular tracers premixed in fluid flows are usually tagged or marked with pulsed lasers, and the flow velocities are derived from the Lagrangian displacements of the tagged molecules. Once the molecular tracers are tagged, the tagged molecules will move with the working fluid. The displacement of the tagged molecules over a prescribed time interval yields the flow velocity.

MTV techniques are usually used to measure one, two, or even three components of flow velocity vectors over a laser-illuminating plane. Depending on how the tracer molecules are tagged, MTV techniques can be sub-categorized as "line-tagging" methods and "grid-tagging" methods. "Line-tagging" methods refer to the MTV measurements that are made by tagging molecular tracers in single or multiple parallel laser beams. Figure 4 shows one example of the "line-tagging" MTV measurements to qualify the unsteady vortex shedding process from a sinusoidally oscillating NACA-0012 airfoil with the phosphorescent triplex of 1-BrNp · Mβ-CD · ROH as the molecular tracer for the measurements [56]. It should be noted that "line-tagging" methods can only provide one component of the velocity vector with its direction normal to the tagged lines. In addition, the estimate of this velocity component usually has an inherent bias error due to the velocity component parallel to the tagged lines. A "multi-time-delay" approach was suggested recently to correct the bias error associated with "line-tagging" MTV measurements [57].

In order to unambiguously measure two components of velocity vectors in a plane, the photoluminescence intensity field from the tagged tracer molecules must have spatial gradients in two, preferably orthogonal, directions [24]. Multiple laser beams from two directions are usually used to generate a grid of intersecting laser lines to "tag" the molecular tracers in the measurement region [23]. Such measurements are usually referred as "grid-tagging" measurements. Figure 5 illustrates one implementation of the "grid-tagging" MTV technique, where Biacetyl was used as the molecular tracer for the measurements [25]. As shown in the Fig. 5, a planar grid of intersecting laser beams, formed from a pulsed excimer laser (20 ns pulse, 308 nm wavelength), was used to turn on the luminescence of Biacetyl molecules that are premixed in a nitrogen flow to examine the flow characteristics at the intake of an IC engine [23]. While Fig. 5a shows the acquired raw images of the tagged Biacetyl molecules acquired right after the laser excitation pulse, the image of the same tagged molecules at 50 µs later is shown in Fig. 5b. Figure 5c gives the corresponding instantaneous flow velocity vectors derived

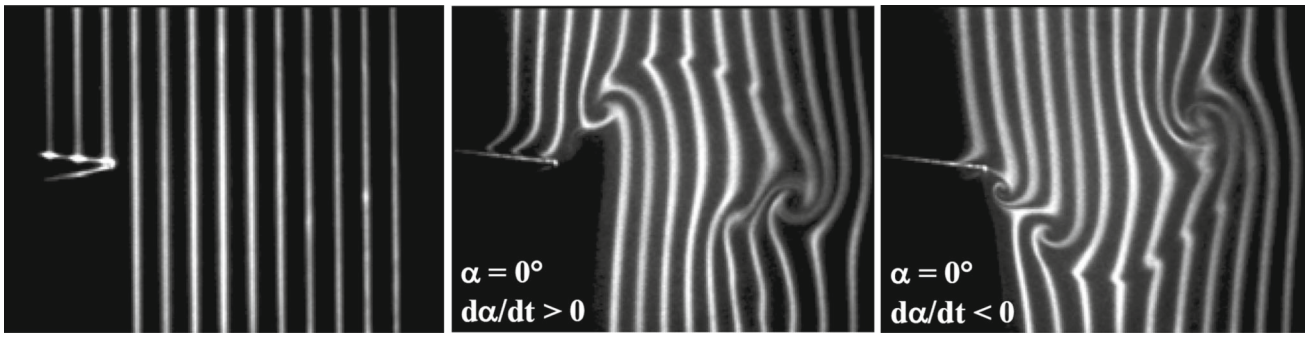

Fig. 4 "Line-tagging" MTV measurements in the wake of an oscillating airfoil [56]

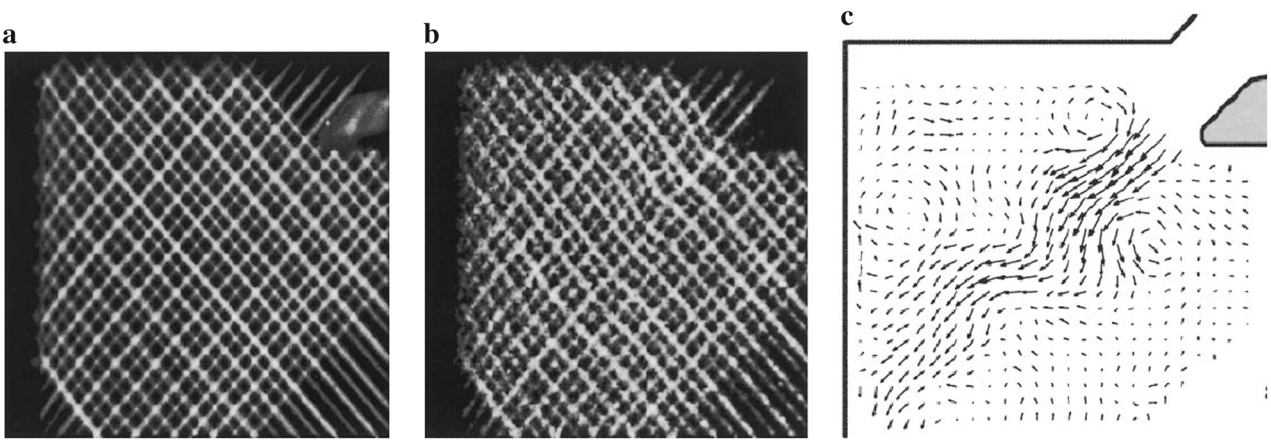

Fig. 5 An example of "grid-tagging" MTV measurement in a gaseous flow [24]. **a** The original tagged grid. **b** Same grid at 50 μs later. **c** Derived velocity vectors

based on the image pair by using a direct spatial correlation method as described in Gendrich and Koochesfahani [24].

While most of the "line-tagging" and "grid-tagging" MTV measurements were conducted to measure either one or two components of the velocity vectors over the regions of interest, accurate results can be obtained for the MTV measurements as long as the flow field is either uni-directional or does not have a significant out-of-plane component. It is well known that the out-of-plane motions in highly three-dimensional flows can seriously impact the accuracy of the "in-plane" velocity measurements using the classic 2-D PIV technique [58,59]. While these effects may not be so serious for MTV measurements [23], a better approach is to use a stereoscopic imaging technique to measure all three components of the velocity vector simultaneously. As shown schematically in Fig. 6, a stereoscopic MTV technique has been developed for achieving simultaneous measurement of all three components of flow velocity vectors [60], which used a similar technical basis of stereoscopic imaging as a stereoscopic PIV technique. It should be noted that, while stereoscopic PIV technique usually requires two laser pulses to illuminate the tracer particles in the fluid flows twice for two PIV image acquisitions, the stereoscopic MTV technique developed by Bohl et al. [60] requires only one pulsed laser to turn the tracer molecules into long-lived glowing markers for the measurements. More recently, Kruger and Gruefeld [37] also developed a stereoscopic MTV technique to simultaneously measure all three components of velocity vectors in a gaseous flow, in which two lasers with different wavelengths were used to provide "write" and "read" laser pulses for the flow velocity measurements.

2.3 Lifetime-based molecular tagging thermometry (MTT) technique

According to Beer's Law for a low concentration of the tracer molecules and unsaturated laser excitation, photoluminescence intensity (both fluorescence and phosphorescence) can be expressed by the following equation [61]

$$I_p = A I_i C \varepsilon \Phi, \tag{1}$$

where I_i is the local incident laser intensity, C the concentration of tracer molecules, ε the absorption coefficient, and

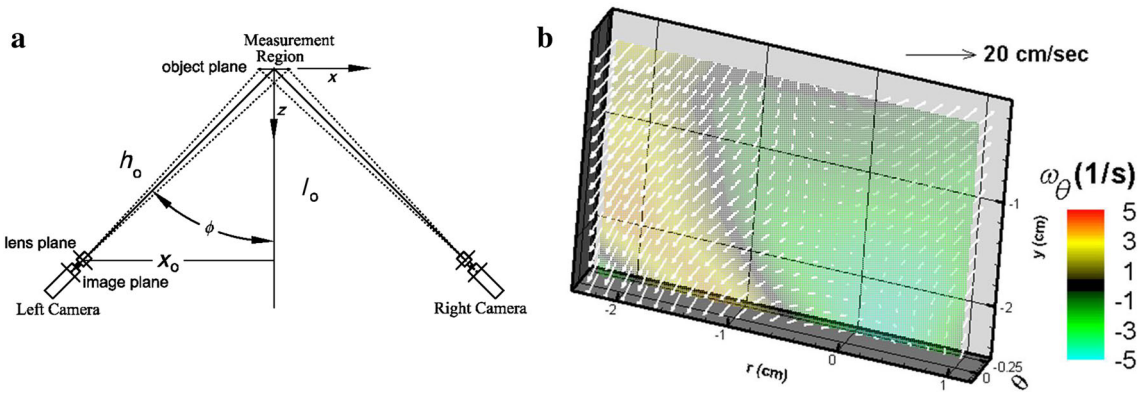

Fig. 6 Schematic of stereoscopic imaging technique and a typical stereoscopic MTV measurement result [60]. **a** Stereoscopic imaging technique. **b** A typical stereoscopic MTV measurement result

Φ the quantum efficiency; A is the fraction of the photoluminescence emission collected by a detector.

According to quantum theory [61], the intensity of a photoluminescence process (either flourescence or phosphorescence) decays exponentially. For simplicity, only a signal-exponential process is considered here. As decribed in Hu and Koochesfahani [19,27], the methodology decribed here is also applicable to a multiple-exponential process.

The photoluminescence intensity decay can be expressed in the form of

$$I_{\mathrm{em}} = I_{\mathrm{o}} \mathrm{e}^{-t/\tau}, \tag{2}$$

where the lifetime τ refers to the time when the intensity drops to 37 % (i.e. 1/e) of the initial intensity I_{o}.

For an excited state, the deactivation processes may involve both radiactive and non-radiactive pathways. The lifetime of the photoluminescence process, τ, is determined by the sum of all the deactivation rates:

$$\tau^{-1} = k_{\mathrm{r}} + k_{\mathrm{nr}}, \tag{3}$$

where k_{r} and k_{nr} are the radiactive and non-radiactive rate constants, respectively. According to photoluminescence kinetics, these rate constants are, in general, temperature-dependent. The temperature dependence of the photoluminescence lifetime is the basis of the lifetime-based MTT technique described here.

The collected photoluminasce intensity can also be determined by integrating Eq. (2) over all times, resulting in

$$I_{\mathrm{p}} = A\tau I_{\mathrm{o}}, \tag{4}$$

where A is the fraction of photoluminescence intensity collected by a digital image detector.

From the Eqs. (1) and (4), it can be deduced that:

$$I_{\mathrm{o}} = I_{\mathrm{i}} \varepsilon \Phi_{\mathrm{p}} C/\tau. \tag{5}$$

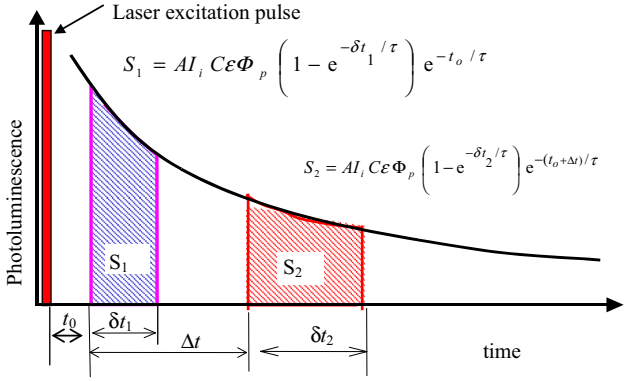

Fig. 7 Schematic of the timing chart for the photoluminescence image acquisition

Now consider capturing the photoluminescence emission by a gated intensified camera where the integration starts at a delay time t_{o} after the laser excitation pulse with a gate period δt. The photoluminescence signal S_{p} collected by the detector is then given by:

$$S_{\mathrm{p}} = A \int_{t_{\mathrm{o}}}^{t_{\mathrm{o}}+\delta t} I_{\mathrm{o}} \mathrm{e}^{-t/\tau} \mathrm{d}t = A I_{\mathrm{i}} C \varepsilon \Phi_{\mathrm{p}} \left(1 - \mathrm{e}^{-\delta t/\tau}\right) \mathrm{e}^{-t_{\mathrm{o}}/\tau}. \tag{6}$$

Figure 7 shows the schematic of the timing chart for the image acquisition for the lifetime-based thermometry technique [19,26]. The photoluminescence signal is imaged at two successive times after each pulsed laser excitation. The first image is detected at the time $t = t_0$ after laser excitation for a gate period δt_1 to accumulate photoluminescence intensity S_1, while the second image is detected at the time $t = t_0 + \Delta t$ for the gate period δt_2 to accumulate photoluminescence intensity S_2. The intensity ratio of the second image intensity (S_2) to the first image intensity (S_1) will be

$$\frac{S_1}{S_2} = \frac{\left(1 - \mathrm{e}^{-\delta t_1/\tau}\right)}{\left(1 - \mathrm{e}^{-\delta t_2/\tau}\right)} \mathrm{e}^{-\Delta t/\tau} \quad \propto \quad f(\tau, \delta t_1, \delta t_2, \Delta t). \tag{7}$$

From Eq. (7), it is evident that the intensity ratio of the two successive photoluminescence images is only a function of the photoluminescence lifetime (τ) and the parameters for the image acquisition (δt_1, δt_2, and Δt); the intensity ratio is not a function of the incident laser intensity (I_i) or the concentration of the tracer molecules (C). The parameters for the image acquisition (δt_1, δt_2, and Δt) are fixed during an experiment. As shown in Fig. 3, since the photoluminescence lifetime is temperature dependent for some molecular tracers [26,53,62,63], the temperature distribution in a fluid flow can be derived from the distribution of the intensity ratio of two photoluminescence images acquired after the same pulsed laser excitation.

For a special case with the two image acquisitions having the same gate period (i.e., $\delta t_1 = \delta t_2$), Eq. (7) can be further simplified as

$$\frac{S_1}{S_2} = \mathrm{e}^{-\Delta t/\tau}. \tag{8}$$

It is suggested that the phosphorescence lifetime can be calculated according to

$$\tau = \frac{\Delta t}{\ln(S_1/S_2)}, \tag{9}$$

resulting in the distribution of the phosphorescence lifetime of the tracer molecules over a two-dimensional domain, thereby, the temperature distribution in the fluid flow as long as the temperature dependence of phosphorescence lifetime is known.

As described above, since the phosphorescence lifetime of some molecular tracers is very temperature sensitive (e.g., 1-BrNp · Mβ-CD · ROH triplex with the temperature sensitivity ranging from 5.0 % per °C at 20 °C to 20.0 % per °C at 50 °C, as shown in Fig. 3), MTT measurements usually have much higher temperature sensitivity than those by using LIF-based thermometry techniques. Furthermore, as indicated in Eq. (7), the intensity ratio (S_1/S_2) is also a function of the controllable parameters (i.e., δt_1, δt_2, and Δt) for the image acqusition. The parameters for the image acqusitions are adjustable and can be optimized for different experimental conditions. Therefore, with the same moleculer tracer, the MTT technique described above can offer an adjustable temperature sensitivity for different applications, simply by adjusting the parameter settings for the image acqusitions. By using this methodology, Hu and Koochesfahani [19] have already developed a novel thermometry technique with an adjustible sensitivity for temperature measurements. As demonstrated in Hu and Koochesfahani [19], with proper parameter settings for the image acqusition, the temperature sensitivity of the MTT measurements can be increased to 18.2 % per °C at $T = 25$ °C, which is about ten times more sensitive than the temperature sensitivity of most commonly used LIF-based thermometry (i.e., about 1.55 % per °C at $T = 25$ °C, with Rhodamine B as the fluorescent dye at $T = 25$ °C, as reported in literature [14,19]). The interplay among various controllable parameter settings for the image acqusition, achievable measurement sensitivities, and accuracies for MTT measurements can provide a great deal of flexibility in optimizing the MTT technique to study various complex thermal flow phenomena.

It should be noted that, since the photoluminescence lifetime is the property of the tracer molecules, it is not affected by the excitation laser intensity or the concentration of the tracer molecules. Therefore, the lifetime-based MTT technique described is a *ratiometric* and *self-calibrated* method, which can eliminate the effects of the temporal or spatial variations of incident laser excitation as well as the effect of non-uniformity of the tracer molecules in the measurement region on the temperature measurement.

As described above, for LIF-based thermometry techniques, the scattering or reflecting laser light may contaminate the acquired fluorescence images, which may result in errors to the temperature measurements. For the lifetime-based MTT measurements, the relatively long phosphorescence lifetime of the molecular tracers allows one to take advantage of the "time axis" in the phosphorescence emission process. As shown in Fig. 7, there is a time delay (t_0) between the excitation laser pulse and the acquisition of the first photoluminescence image for the image acquisition. Since the scattering or reflecting laser light only exists for the duration of the excitation laser pulse, the strong scattering/reflection of the intense excitation source can be eliminated effectively by simply putting a small time delay between the laser excitation pulse and the starting time for MTT image acquisitions.

It should also be noted that, to implement the lifetime-based MTT technique, only one laser pulse is required to excite or tag the tracer molecules for each instantaneous temperature field measurement. The two successive acquisitions of the photoluminescence images of the excited or tagged tracer molecules can be achieved using a dual-frame intensified digital camera. Compared to the two-dye LIF approach [14,16], the single-dye two-emission-band LIF method ([17] and dual-wavelength LIF approach [18] described above, which usually requires two cameras for image acquisition and/or two laser pulses with different wavelength for the excitation for each instantaneous temperature field measurement, the lifetime-based MTT technique is much easier to implement and can significantly reduce the burden on the instrumentation and experimental setup needed for the measurements.

2.4 Molecular tagging velocimetry and thermometry (MTV&T) technique for simultaneous velocity and temperature measurements in fluid flows

Although there is an extensive literature on the measurements of either velocity components or temperature in many types of fluid flows, the studies involving simultaneous flow velocity and temperature measurements are very limited. Earlier work about the simultaneous flow velocity and temperature measurements in fluid flows concerned single-point simultaneous acquisition of flow velocity and temperature at the limited points of interest. For example, taking advantage of the temperature dependence of fluorescence emission, a combined laser induced fluorescence (LIF) and laser Doppler anemometry (LDA) technique was used by Lemoine et al. [64] to conduct both temperature and velocity measurements at the points of interest in a turbulent heated jet. More recently, whole-field diagnostic techniques such as PIV and PLIF techniques are combined to achieve simultaneous measurements of flow velocity and temperature distributions to quantify the characteristics of complex thermal flows [14,65]. It should be noted that, when PIV is combined with PLIF, complications such as the influence of laser light absorption/scattering by the seed particles on the LIF signal need to be carefully considered. For the combined PIV/PLIF technique, at least two cameras with various optical filters are required to record the particle scattering and LIF signals separately. A very careful image registration or coordinate mapping procedure is also required in order to get the quantitative spatial relation between the simultaneous velocity and temperature measurements. A digital particle image velocimetry/thermometry (DPIV/T) technique has also been developed recently, which uses thermochromic liquid crystal (TLC) encapsulated microspheres as the tracer particles [66,67], to achieve simultaneous flow velocity and temperature measurement in fluid flows. Since particles are used also for temperature measurements (e.g., TLC encapsulated microspheres), additional considerations are also required about the thermal response of the particle tracers.

As described above, the lifetime-based MTT technique requires imaging the phosphorescence signal at two successive times, which is the same as in MTV measurements. MTV and MTT techniques can be easily combined to result in a so-called MTV&T technique [26], which is capable of achieving simultaneous measurements of velocity and temperature distributions in fluid flows. The MTV&T technique, which is a completely *moelcule-based* flow diagnostic technique, has the same capabilitiese as a PIV/PLIF combined technique [15,64], but can significantly reduce the burden on the instrumentation and experimental setup.

In MTV&T measurements, the tracer molecules premixed in the working fluid are "tagged" or "excited" using multiple pulsed laser beams in either multiple lines or a grid pattern. Two successive photoluminescence images of the tagged molecules are acquired after each laser excitation pulse. The movements of the tracer molecules during the time intervial between the two image acquisitions are initially used to derive the flow velocity vectors. Then, the velocity vectors are used to find the corresponding "tagged" tracer molecules in the two photoluminscent images. The simultaneous temperature measurement is achieved by taking advantage of the temperature dependence of the phosphorescence lifetime, which is estimated from the phosphorescence intensity ratio of the same "tagged" molecules in the two interrogations. This process will completely eliminate the ambiguities for temperature measurements due to the spatially varying incident laser excitation and non-uniform molecular tracer concentration in the measurement region as well as the displacement of the tracer moelcules during the time interval of the two image acqusitions.

The implementation of the molecular tagging techniques described above is demonstrated by three examples given in the following section.

3 Applications of MTV and MTT techniques for complex thermal flow studies

3.1 To examine the thermal effects on the wake instabilities behind a heated cylinder

The heat transfer process from a circular cylinder (i.e., a bluff body) to surrounding fluid is of great importance due to its fundamental nature as well as many related engineering applications. Despite its simple shape, a circular cylinder generates a wake flow that is dynamically complex. By varying the Reynolds number, a variety of flow patterns and vortex shedding characteristics in the wakes of circular cylinders have already been observed. Extensive reviews about the effects of Reynolds number on the flow pattern in the wake of an unheated circular cylinder are available in the literature [68–72]. The wake behavior behind a heated cylinder is physically more complicated due to the thermal effects added to the viscous phenomena. As described in the textbook by Incropera and DeWitt [73], the heat transfer from a heated cylinder to surrounding fluid can be either forced convection, mixed convection, or pure free convection, depending on the ratio between the thermally-induced buoyancy force to the inertial force, characterized by the Richardson number ($Ri = Gr/Re^2$, where Gr is the Grashof number and Re is the Reynolds number). In forced convection ($Ri \ll 1$), where the effect of thermally-induced buoyancy force is negligible, heat transfer is a function of Reynolds number and Prandtl number (Pr). In free convection ($Ri \gg 1$), where the flow inertial force is negligible, heat transfer is a function of Grashof number (Gr) and Prandtl number (Pr). In mixed

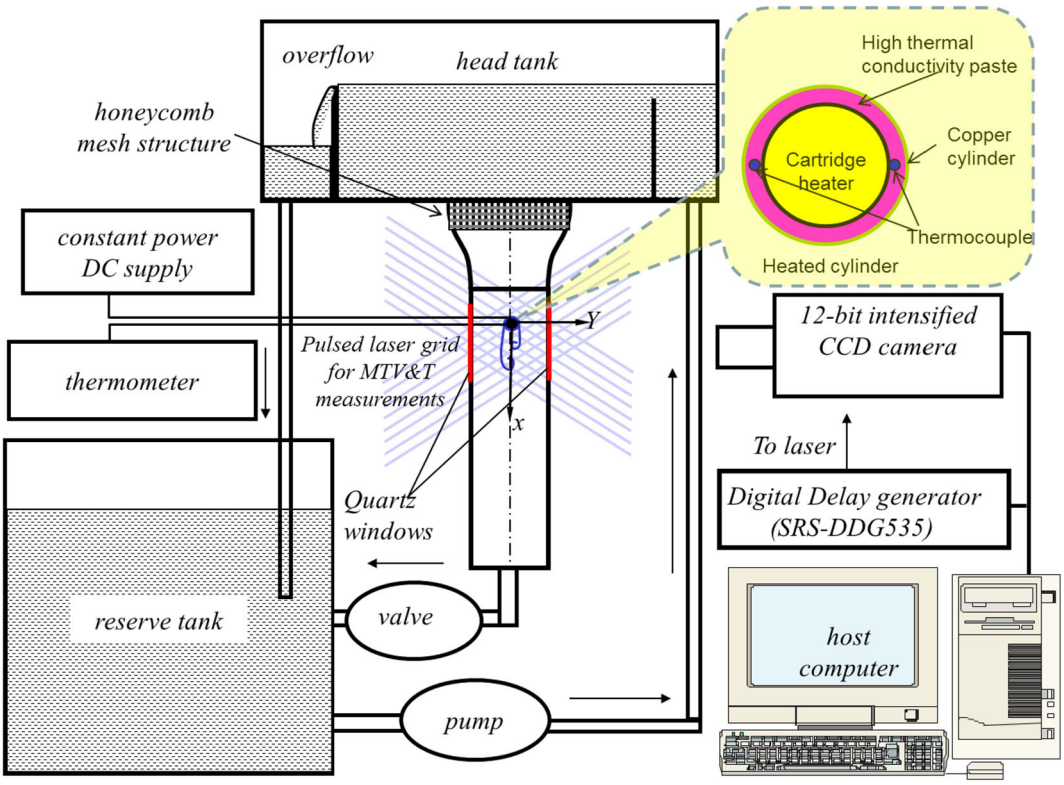

Fig. 8 Experimental setup to examine the thermal effects on the wake insatiability behind a heated cylinder [27]

convection, both forced convention and free convection are important, and heat transfer is a function of Grashof number (Gr), Reynolds Number (Re), and Prandtl number (Pr), as well as the approaching forced flow direction.

By using the MTV&T technique described above, a comprehensive study has been conducted to quantify the unsteady heat transfer process from a heated circular cylinder to the surrounding fluid flow and to examine the thermal effects on the wake instabilities behind the heated cylinder operating in the mixed and forced convection regime [27]. Figure 8 shows the schematic of the experimental setup used for the experimental study. The 1-BrNp · Mβ-CD · ROH triplex premixed with water flow was used for the MTV&T measurements. The water flow was held at a pre-selected temperature by using a constant temperature bath. A constant head tank, which is filled from the reservoir tank using an electric pump, was used to maintain a steady inflow condition during the experiments. A copper tube, which was heated by using a rod cartridge heater placed inside the tube, was used as the test cylinder for the experimental study. By adjusting the incoming flow velocity and the temperature of the heated cylinder, the heat transfer process from the heated cylinder to the surrounding flow would be in natural, mixed, and forced heat convection regimes.

As shown schematically in Fig. 8, a Lambda-Physik XeCl excimer laser (wavelength of 308 nm, energy 100 mJ/pulse, pulse width 20 ns) with appropriate optics was used to generate a grid of intersecting laser lines to "tag" the 1-BrNp · Mβ-CD · ROH tracer molecules premixed in the working fluids. A gated intensified camera (PCO DICAM-Pro) with a fast-decay phosphor (P46) was used for the image recording. The camera was operated in a dual-frame mode, where two full-frame images of phosphorescence were acquired in quick succession from the same laser excitation pulse. The laser and the camera were synchronized using a digital delay generator (SRS-DDG535), which controlled the timing of the laser sheet illumination and the intensified camera data acquisition. The phosphorescence images captured by the camera were subsequently transferred to a host computer for image processing and data analysis.

Figure 9 shows typical MTV&T measurements to reveal the unsteady heat transfer process from the heated cylinder to surrounding fluid flow at the test condition of $Re = 130$ and $Ri = 0.31$. As described above, 1-BrNp · Mβ-CD · ROH tracer molecules were tagged by multiple pulsed laser beams in a grid pattern. Upon the pulsed laser excitation, the 1-BrNp·Mβ-CD · ROH tracer molecules give off long-lifetime phosphorescence emission, serving as the glowing markers for the flow measurements. The movements of the glowing tracer molecules are imaged twice after the same laser pulse. While Fig. 9a, b show the initial image of the tagged molecules in the measurement region and their sub-

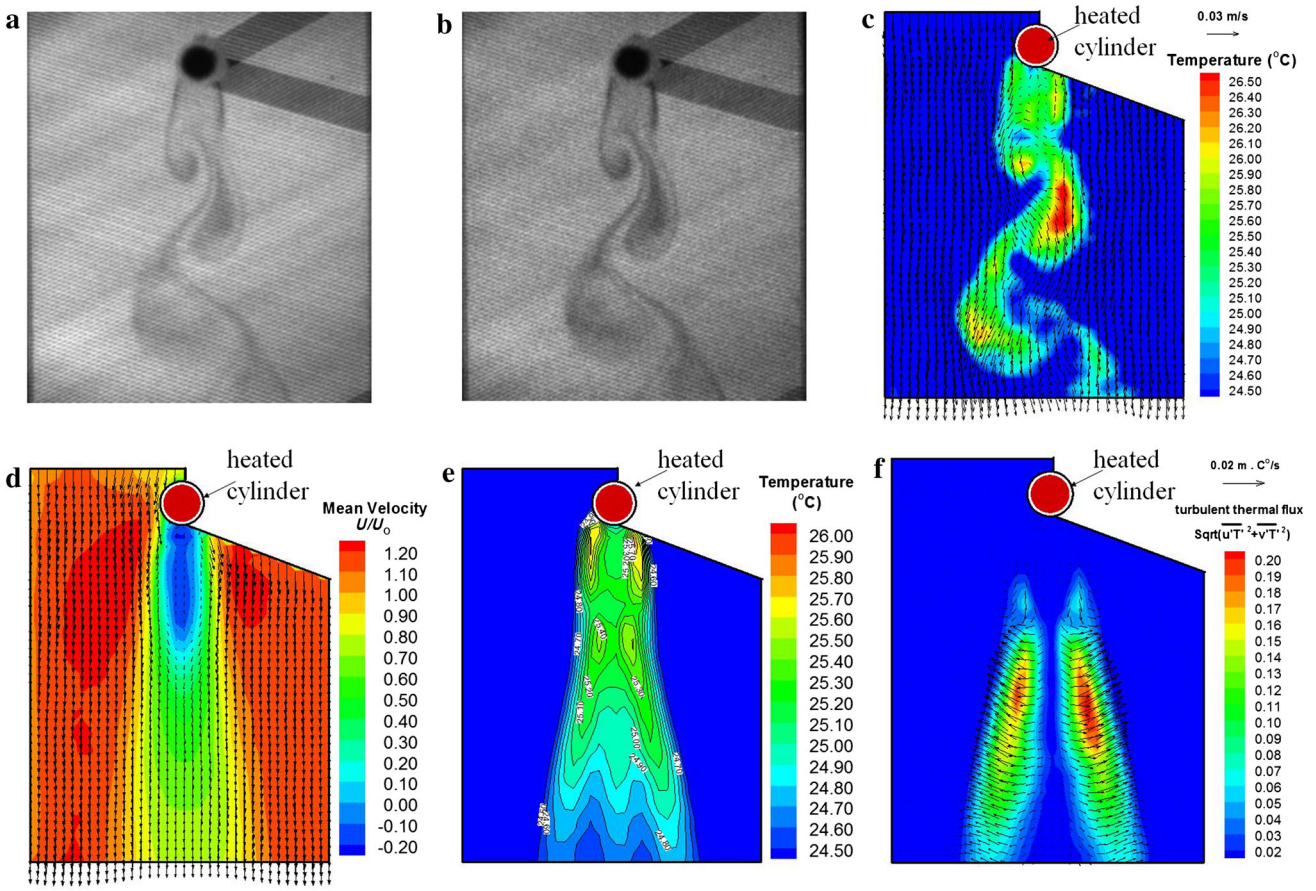

Fig. 9 Typical MTV&T measurement results in the wake flow of a heated cylinder [27]. **a** Grid image at 0.5 ms after the laser excitation pulse. **b** The same tagged molecules at 5.0 ms later. **c** Velocity and temperature fields derived from the image pairs. **d** Ensemble-averaged velocity distribution. **e** Ensemble-averaged temperature field. **f** Turbulent thermal flux vectors

sequent evolution after a time delay of 5 ms, Fig. 9c gives the resultant simultaneous velocity and temperature distributions derived from the image pair. Based on a cinema sequence of instantaneous MTV&T measurements as those shown in Fig. 9c, the ensemble-averaged velocity and temperature distributions in the cylinder wake were calculated, and the results are shown in Fig. 9d, e, respectively. Since the velocity and temperature fields were measured simultaneously, the correlation between the velocity and temperature fluctuations can also be calculated to generate the distribution of the mean turbulent heat flux $\overline{u_j' T_j'}$ in the wake of the heated cylinder, as shown in Fig. 9f.

During the experiments, the velocity and temperature of the approach flow were held constant. By adjusting the surface temperature of the heated cylinder, the corresponding Richardson number (i.e., $Ri = Gr/Re^2$) was varied between 0.0 (unheated) and 1.04, resulting in a change in the heat transfer process from forced convection regime to mixed convection regime. Figure 10 shows the typical instantaneous MTV&T measurement results at different Richardson number levels. It can be seen clearly that, with increasing temperature of the heated cylinder (i.e., increasing Richardson number), significant modifications of the wake flow pattern and wake vortex shedding process were clearly revealed. When the Richardson number was relatively small (i.e., in the forced convection regime with $Ri \leq 0.3$), the vortex shedding process in the wake of the heated cylinder was found to be quite similar to that of an unheated cylinder. As the Richardson number increased to $Ri \geq 0.3$, the wake vortex shedding process was found to be "delayed", with the wake vortex structures beginning to shed much further downstream. As the Richardson number approached unity ($Ri \geq 0.7$), instead of having "Karman" vortices shedding alternately at the two sides of the heated cylinder, concurrent shedding of smaller vortex structures was observed in the near wake of the heated cylinder.

Based on the MTV&T measurement results such as those shown in Figs. 9 and 10, the unsteady heat transfer process from the heated cylinder to the surrounding fluid flow at different heat transfer regimes can be revealed very clearly and quantitatively. This is essential to elucidate the underlying physics and to improve our understanding about the

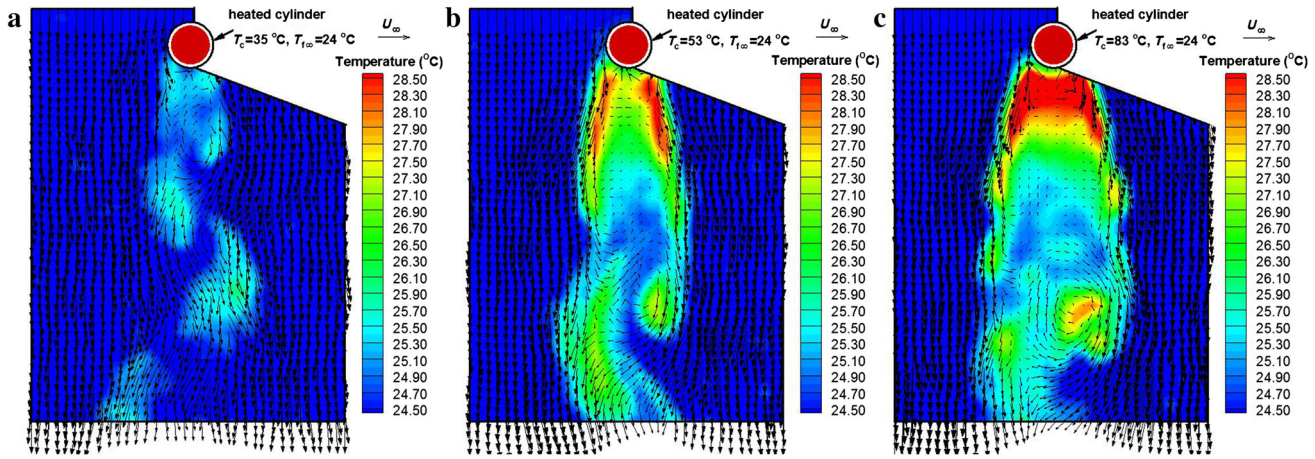

Fig. 10 Instantaneous MTV&T measurement results at different Richardson numbers. **a** $Ri = 0.19$. **b** $Ri = 0.50$. **c** $Ri = 1.04$

thermal effects on the wake instabilities behind the heated cylinder operating in natural, mixed, and forced heat convection regimes. Further details about the implementation of the MTV&T technique and the significant findings derived from the MTV&T measurement results as those given above to examine the thermal effects on the wake instabilities behind the heated cylinder can be found in Hu and Koochesfahani [26,27].

3.2 To quantify the unsteady heat transfer and phase changing process within micro-sized icing water droplets pertinent to aircraft icing phenomena

Aircraft icing is widely recognized as a significant hazard to aircraft operations in cold weather. When an aircraft or rotorcraft flies in a cold climate, some of the super cooled droplets will impact and freeze on exposed aircraft surfaces to form ice shapes. Ice may accumulate on every exposed frontal surface of an airplane, not only on the wing, propeller and windshield but also on the antennas, vents, intakes, and cowlings [74]. Ice accumulation can degrade the aerodynamic performance of an airplane significantly by increasing drag while decreasing lift [75]. In moderate to severe conditions, an airplane can become so iced up that continued flight is impossible [76]. The airplane may stall at much higher speeds and lower angles of attack than normal. It can roll or pitch uncontrollably, and recovery may be impossible. Ice can also cause engine stoppage by either icing up the carburetor or, in the case of a fuel-injected engine, blocking the engine's air source [77–79]. The importance of proper ice control for aircraft operation in cold climate was highlighted by many aircraft crashes in recent years like the Continental Connection Flight 3407 crashed in Buffalo, New York due to ice buildup on its wings killing all 49 people aboard and 1 person on the ground as the plane hit a residential home on February 14, 2009. Military aircraft are not immune from icing hazards either. The military operates airfields across the world, many of which require de-icing/anti-icing to be conducted if operations are to continue during cold weather. Icing has been found to causes military mission delays during ground de-icing of aircraft and even mission cancellations and abortions because of forecast or actual in-flight icing [80,81]. Regardless of the aircraft type being supported, the methods of de-icing/anti-icing and the concerns that accompany it remain the same. While research progress has been made in recent years in providing better understanding about aircraft icing phenomena, aircraft icing remains as an important unsolved problem at the top of the National Transportation Safety Board's most wanted list of aviation safety improvements.

Due to lack of knowledge, current ice prediction tools and ice protection system designs for aircraft icing mitigation make use of simple classical models which ignore many of the details of the interaction of the three-phase flows (i.e., air, water, and ice) that are responsible for the ice formation and accretion [74,75,77,79]. Many important micro-physical processes associated with aircraft icing phenomena, such as transient behavior of surface water droplets and film/rivulet flows, unsteady heat transfer process within icing water droplets/film flows, and phase change of supercooled water droplets/film flows over smooth/rough surfaces, are still unclear. Advancing the technology for safe and efficient aircraft operation in atmospheric icing conditions requires a better understanding of the important microphysical phenomena pertinent to aircraft icing phenomena. By using the lifetime-based MTT technique described above, Hu and his group conducted a series of icing physics studies in recent years in order to improve our understanding about the important microphysical processes pertinent to aircraft icing phenomena [11,21,82,83].

Figure 11 shows the schematic of the experimental setup used in the experimental study to quantify the transient icing

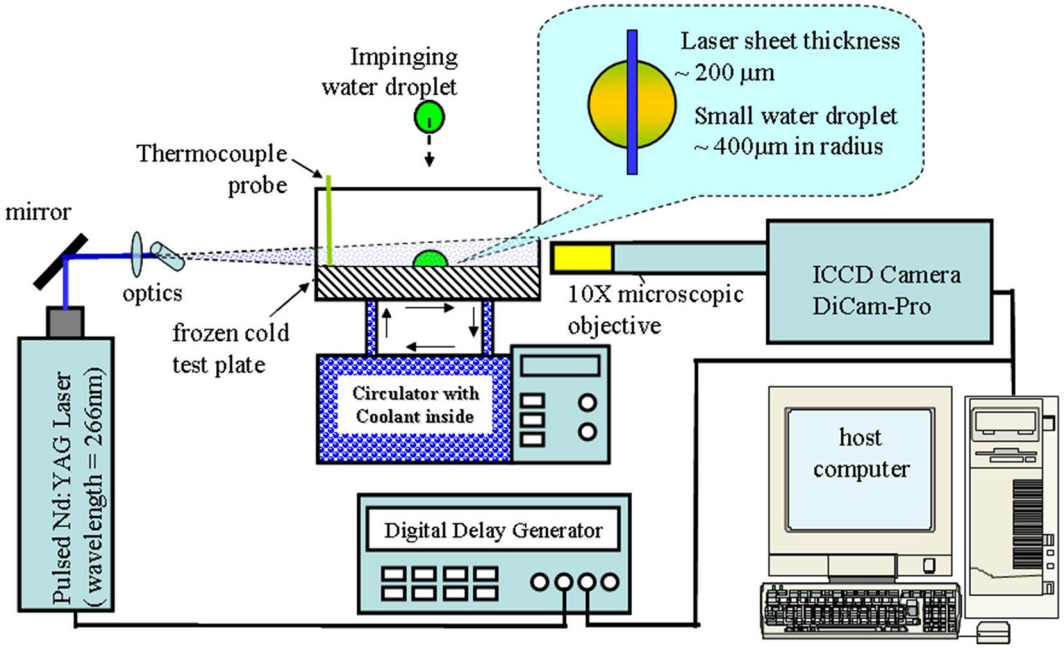

Fig. 11 Experimental setup for icing droplet study

process within small water droplets impinging onto a frozen cold test plate, which is pertinent to the ice formation and accreting process as water droplets impinging onto icing aircraft wings [11,83]. As shown schematically in Fig. 11, a droplet generator was used to generate micro-sized water droplets to impinge onto a test plate. The temperature of the test plate, monitored by using a thermocouple, was kept constant at a pre-selected low temperature level by using a Constant Temperature Bath Circulator. A laser sheet from a pulsed Nd:YAG laser at a quadrupled wavelength of 266 nm was used to tag the 1-BrNp · Mβ-CD · ROH molecules premixed in the water along the middle plane of the small water droplets. A dual-frame intensified CCD camera with a 10× microscopic objective was used to capture the phosphorescence images at two successive times after the same laser excitation pulse.

Figure 12 shows a typical pair of the acquired phosphorescence images for the MTT measurements and the instantaneous temperature distribution inside the water droplet derived from the phosphorescence image pair, which were taken 5.0 s later after the water droplet (initial temperature 20.5 °C) impinged onto the cold test plate (T_w = 5.0 °C). As shown in Fig. 12a, b, since the time delays between the laser excitation pulse and the phosphorescence image acquisitions can effectively eliminate scattered/reflected light and any fluorescence from other substances (such as from the surface of the test plate) in the measurement region, the phosphorescence images of the water droplet are quite "clean" even though no optical filter was used for the phosphorescence image acquisition. As described above, Eq. (9) can be used to calculate the phosphorescence lifetime of the tagged molecules on a pixel-by-pixel basis, which results in a distribution of the phosphorescence lifetime over a two-dimensional domain. With the calibration profile of phosphorescence lifetime vs. temperature as shown in Fig. 3, a two-dimensional, instantaneous temperature distribution within the water droplet can be derived from the phosphorescence image pair, and the results are shown in Fig. 12c. Based on a time sequence of the measured transient temperature distributions within the water droplet as shown in Fig. 12, the unsteady heat transfer process within the convectively-cooled water droplets was revealed quantitatively. It should also be noted that, in addition to measuring the temporally-and-spatially-resolved temperature distribution within the small water droplet, other quantities, such as the volume, height, contact area, and the contact angle of the water droplet over the test plate at different test conditions can also be determined simultaneously based on the "clean" MTT images of the water droplet such as those shown in Fig. 12.

The lifetime-based MTT technique was also used to quantify the transient phase changing phenomena inside a micro-sized icing droplet over a frozen surface in order to improve our understanding about the ice formation and accretion process as water droplets impinging onto frozen cold aircraft wings. Figure 13 shows typical phosphorescence images and corresponding temperature distributions of the remaining liquid water within a small icing water droplet after it impinged onto a frozen cold test plate. In the images, the "brighter" region (due to the expulsion of

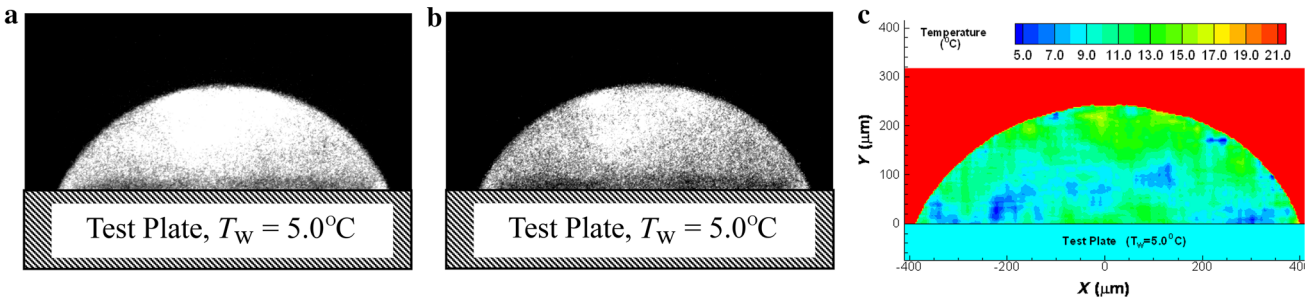

Fig. 12 A typical MTT measurement result with $T_W = 5.0\,°C$. **a** The first phosphorescence image acquired at 0.5 ms after the laser pulse. **b** The second phosphorescence image acquired at 3.5 ms same laser pulse. **c** Instantaneous temperature distribution derived from the image pair

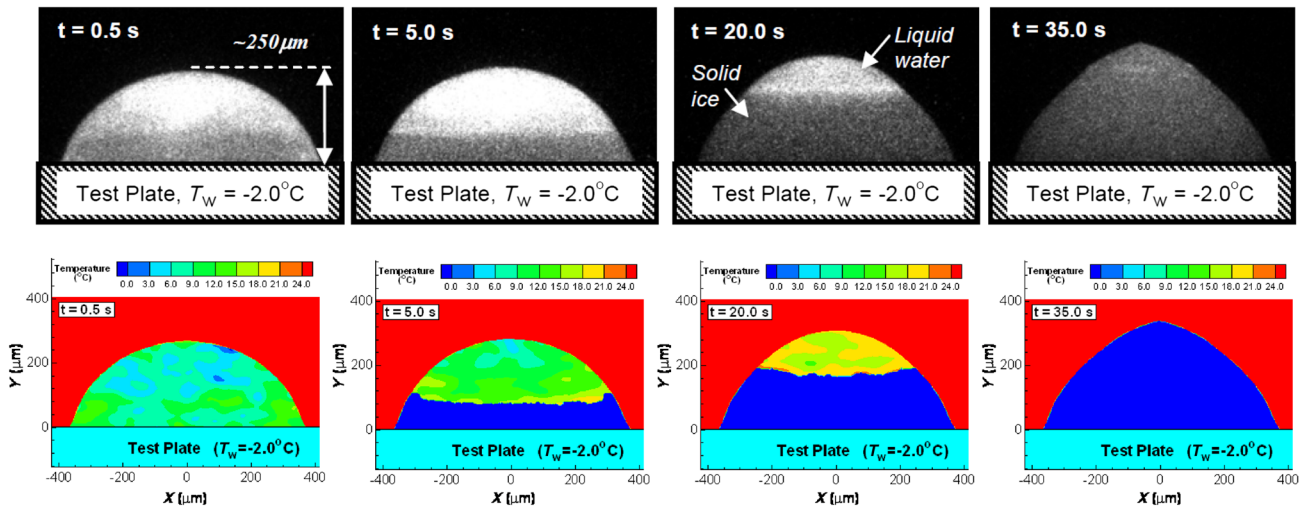

Fig. 13 MTT measurements of the phase changing process within an icing water droplet [11]. The *lower set* of four figures shows the measured temperatures within a freezing water surface bead, *blue* is ice and the *colored regions* are liquid water with temperatures ranging from freezing (*blue*) to warmer than freezing (*green* to *red*)

the molecular tracers during freezing) in the upper portion of the droplet represents the liquid phase—water; while the "darker" region at the bottom indicates the solid phase—ice. It can be clearly seen that the liquid water at the bottom of the droplet was frozen and turned to solid ice rapidly, while the upper portion of the droplet was still in the liquid state. As time goes by, the interface between the liquid phase water and solid phase ice was found to move continuously upward. As a result, the droplet was found to grow upward with more and more liquid phase water changing to solid phase ice. At about 35 s after the droplet impinged onto the cold test plate, the droplet was found to turn completely into a solid ice crystal. Based on the time sequence of the MTT measurements as those shown in Fig. 13, the time evolution of the unsteady heat transfer and phase changing process within the small icing droplet are revealed clearly and quantitatively. The underlying physics elucidated from the quantitative MTT measurement results such as those shown in Figs. 12 and 13 could lead to a better understanding of the important micro-physical processes pertinent to aircraft icing phenomena. This can be used to improve current icing accretion models for more accurate prediction of ice formation and accretion processes on aircraft as well as to develop more effective and robust anti-/de-icing strategies to ensure safer and more efficient operation of aircraft in cold weather. Further information about the icing physics experiments and the discussions about the icing physics revealed from the MTT measurements are available in the references [11,21,82].

3.3 To use MTV and MTT techniques to achieve simultaneous measurements of droplet size, velocity, and temperature of "in-flight" droplets in a spray flow

It is well known that the process of breaking up or atomization of liquid fuel into droplets in the form of a fine spray plays a pivotal role in improving energy efficiency and suppressing

pollutant formation for various gas turbines and IC engines, while meeting the operability requirements of the particular application. A detailed definition of the dynamic and thermodynamic behavior of fuel droplets in a spray flow is essential for the optimization of a liquid fuel injector/atomizer in order to maximize energy efficiency, minimize pollutant emissions, and meet the operability requirements of the particular application.

Among various parameters of interest in characterizing fuel spray flows, droplet temperature is one of the least investigated due to the lack of proper measurement techniques. Droplet temperature is actually a very important index associated closely with the atomization and evaporation processes of liquid fuel droplets. The processes play significant roles by controlling the distribution of the fuel droplets, thus, the local fuel/air ratio in combustion chambers. This ratio can be directly related to the global efficiency of combustion and to the formation of pollutants.

A number of experimental studies have been conducted in recent years to use LIF-based thermometry to achieve non-intrusive measurements of droplet temperature in spray flows. For example, Lavieille et al. [17] developed a two-color LIF imaging technique to measure the temperature of evaporating and combusting droplets. In addition, Castanet et al. [84] conducted an experimental study to examine the energetic budget of a monodisperse ethanol droplet stream injected in the thermal boundary layer of a vertical heated plate. While the droplet size reduction is measured using a light scattering technique (interferential method) in order to characterize the evaporation, the droplet mean temperature is measured by using the two-color LIF technique. By using the MTV and MTT techniques described above, an explorative study has been conducted recently to achieve simultaneous measurements of droplet size, flying velocity, and instantaneous temperature of inflight droplets in order to characterize the dynamic and thermodynamic behaviors of droplets in spray flows.

Figure 14 shows a typical measurement result of the explorative study, which can be used to demonstrate the feasibility of utilizing the MTV and MTT techniques to achieve simultaneous measurements of droplet size, velocity, and temperature of flying fuel droplets in spray flows. For the experimental study, a droplet generator was used to inject micro-sized droplets with an initial temperature of $T_{\text{Droplet}} = 11.2\,^{\circ}\text{C}$ into ambient airflow. The temperature of the ambient air was keep constant at $T_{\text{Air}} = 22.0\,^{\circ}\text{C}$ during the experiments. The micro-sized droplets are heated up as they are injected into the airflow, which is pertinent to the atomization and evaporation processes of liquid fuel droplets injected into combustion chambers. A pulsed Nd:YAG at quadrupled wavelength of 266 nm was used to tag phosphorescent triplex (1-BrNp·Mβ-CD·ROH) molecules premixed within the liquid fuel. A dual-frame intensified CCD camera was used to capture the phosphorescence images at two successive times after each laser excitation pulse. For the measurement results given in Fig. 14, the measurement window is located at 100 mm downstream of the droplet generator exit. While the first phosphorescence image was taken at 0.23 ms after the excitation laser pulse with the exposure time of 0.1 ms, the second phosphorescence image was acquired at 1.1 ms later with the same exposure time. Based on the acquired phosphorescence images of the droplets given in Fig. 14, the droplet sizes can be determined based on a predetermined scale ratio between the image plane and the object plane (i.e., $D_{\text{Droplet}} \approx 450\,\mu\text{m}$ for the case shown in Fig. 14). The displacements of the droplets between the two acquired phosphorescent images can be used to determine the flying/moving velocity of the droplets (i.e., $V_{\text{Droplet}} \approx 2.03$ m/s for the case shown in Fig. 14). The temperature of the "in-flight" water droplets can also be derived simultaneously by taking advantage of the temperature dependence of phosphorescence lifetime, which is estimated from the phosphorescence intensity ratio of the droplets in the two interrogations (i.e., $T_{\text{Droplet}} \approx 12.0\,^{\circ}\text{C}$ for the case shown in Fig. 14).

With the quantitative information about the droplet size, flying velocity, and temperature of the "in-flight" droplets derived from the MTV/MTT measurements as that shown in Fig. 14, the dynamic and thermodynamic behaviors of the fuel droplets in spray flows can be revealed in great detail. Such quantitative measurements are very desirable to improve our understanding about the atomization and evaporation processes of the fuel droplets injected from fuel injectors/atomizers in the combustion chambers of gas turbines and IC engines. A better understanding about the important microphysical processes will enable us to optimize the fuel injectors/atomizer for improved energy efficiency and reduced pollutant formation.

3.4 On the resolution limitations and uncertainty of MTV/MTT measurements

The MTV and MTT techniques described above, like most other measurement techniques, do not give information at a "point". They provide spatially-averaged velocity and temperature of a molecularly tagged region. Similar to the PIV technique, the effective spatial resolution of MTV measurements is given by the sum of the interrogation window size and the measured Lagrangian displacement. Clearly, it would require tagging regions and selecting interrogation windows consistent with the scales to be resolved in order to obtain resolved data to quantify the small scale thermal/flow structures. While the best spatial resolution would be set by the diffraction limitations of optics used to generate the tagging pattern and the resolution characteristics of image detection, the selection of the interrogation window would often involve a choice between the spatial resolution of MTV/MTT mea-

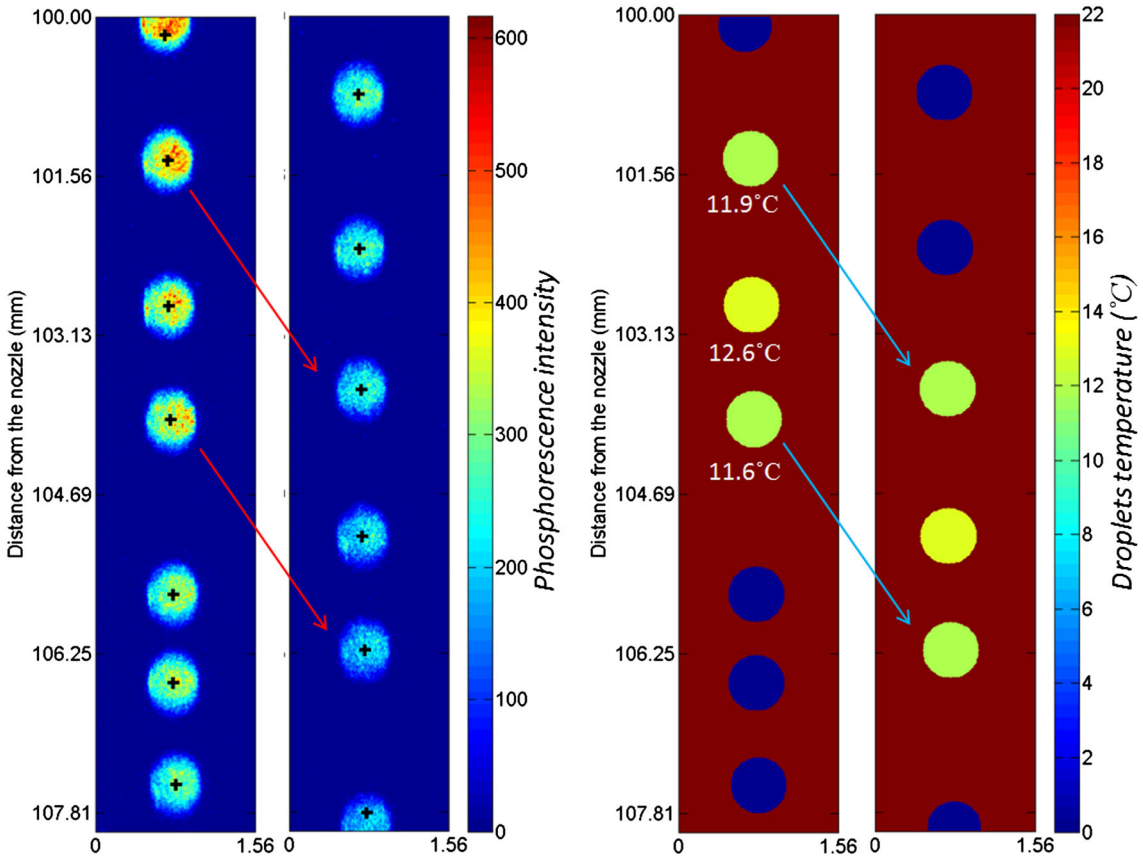

Fig. 14 A typical MTV/MTT measurement result to achieve simultaneous measurements of droplet size, velocity, and temperature of "in-flight" droplets [85]

surements versus the accuracy levels of the measurements. The temporal resolution of the MTV/MTT measurements would be determined by the time delay between the acquired phosphorescence image pair. The choice of the time delay would also affect the accuracy of the velocity data (i.e., larger Δt leads to larger Lagrangian displacement of tagged molecules) and the temperature estimation through Eq. (9).

The uncertainty levels of MTV measurements depend on many parameters, such as the signal-to-noise ratio in the MTV image pair, the intersection angle and width of the laser beams used for tagging, and the size of the source window in the correlation process, which have been systematically studied and documented in Ref. [24]. The accuracy of temperature measurements using MTT technique is mainly affected by two factors, i.e., (1) the noise levels in the two acquired phosphorescence images leading to noise in the estimated lifetime, and (2) the inaccuracies in the identification of the region in the second phosphorescence image corresponding to the original tagged region in the first image.

The accuracy in the determination of lifetime from Eq. (9), and the resultant accuracy in temperature measurement, is directly affected by the noise levels in the two acquired phosphorescence signals S_1 and S_2. Even though 12-bit cameras are widely used for MTV/MTT measurements [11,19,21,27,85], the actual image noise at each pixel, characterized by the standard deviation of the signal, is usually in the 3 % range. This noise level is related to the CCD depth of field and the intensifier stage of the CCD. As suggested by Ballew and Demas [86], the accuracy in calculating the phosphorescence lifetime can be estimated by

$$\frac{\sigma_\tau}{\tau} = \frac{1}{\ln\left(S_1/S_2\right)}\sqrt{\left(\frac{\sigma_{S1}}{S_1}\right)^2 + \left(\frac{\sigma_{S2}}{S_2}\right)^2}, \tag{10}$$

where σ_{S1}, σ_{S2}, and σ_τ are the standard deviations of S_1, S_2, and τ, respectively. As described in Hu and Koochesfahani [26], the aforementioned 3 % phosphorescence signal accuracy at each pixel will result in a lifetime measurement accuracy of about 4 % and an instantaneous temperature error of 0.8 °C (using the lifetime temperature sensitivity of 5.0 °C at 20 °C for reference). Since this error is unbiased, it can be substantially reduced by averaging over neighboring pixels. Assuming statistical independence, the error can be reduced by the factor $1/\sqrt{N}$ where N is the number of pixels in the interrogation window. For example, when interrogation windows of 32 pixels×32 pixels are used for the image processing of MTT measurements, the instantaneous

measurement error due to the noise in the phosphorescence images would be much less than 0.1 °C [26].

Unlike LIF-based thermometry techniques, the lifetime-based MTT method described here is a Lagrangian approach. The molecular region tagged in the first image convects to a new region in the second image according to its Lagrangian displacement over the time delay between the two images. This new region in the second phosphorescence image needs to be identified correctly in order to accurately determine the phosphorescence lifetime. Since the effects of mass diffusion are usually negligible due to the short time delay between the two image acquisitions, the location of the new region would be determined solely on the basis of advection by the flow. In MTT image processing, for each interrogation window in the first phosphorescence image, the identification of its corresponding region in the second phosphorescence image was based on the Lagrangian displacement by the amount already determined by the correlation method in MTV. This is a first-order method that uses a linear displacement model consistent with small Lagrangian displacements (i.e., small time delay between images) and small distortion of the tagged regions due to velocity gradients. Higher order processing methods can, in principle, be developed to take image distortions into account [26]. It is noteworthy that, thermally induced distortions in the MTV/MTT measurement windows may cause errors in determining the positions of the measurement points. The effects could become significant when the scale of the thermally induced distortions is comparable to the spatial resolution of the MTV/MTT measurements, for example, in cases with very large temperature gradients and/or very high spatial resolution.

A study was performed by Hu and Koochesfahani [26] to investigate the temperature measurement errors caused by the distortions due to velocity gradients and the inaccuracy of the velocity measurement itself. In MTT image processing to calculate the fluid temperature, they used the regions in the second phosphorescence image that were deliberately displaced an additional ±1 pixel (i.e., 25 % of maximum displacement) relative to the actual location computed by MTV. The "induced" mismatch was found to result in a temperature error of about 0.1 °C for the test conditions. They also reported a maximum uncertainty of 0.23 °C in the temperature measurements, which is the total uncertainty in MTT measurements that accounts for all the effects discussed above. More recently, Ke et al. [87] also conducted an investigation to estimate the errors in the temperature and velocity measurements by using MTT and MTV techniques. They reported estimated errors of approximately 0.1–0.3 °C and 0.1–0.2 pixels in the temperature and velocity measurements, respectively. It was also found by Ke et al. [87] that it is very difficult, if not impossible, to simultaneously minimize the errors in the displacement and temperature measurements. The optimized experimental parameters for MTV and MTT measurements are usually chosen on a case-by-case basis.

4 Conclusions

A comprehensive review on the recent progress in the development of MTV and MTT techniques is reported in the present study. The MTV and MTT are *molecule-based* flow diagnostic techniques, which are capable of achieving both qualitative flow visualization of thermally induced flow structures and quantitative measurements of velocity and temperature distributions in fluid flows. The MTV and MTT techniques can also be easily combined to result in a so-called MTV&T technique, which is capable of achieving simultaneous measurements of velocity and temperature distributions in fluid flows. As a completely *molecule-based* flow diagnostic technique, the MTV&T technique has the same capabilities as a PIV/PLIF combined technique, but can significantly reduce the burden on the instrumentation and experimental setup.

Instead of using tiny particles, the molecular tagging techniques (i.e., MTV, MTT, and MTV&T) utilize specially designed phosphorescent molecules as the tracers for the whole-field flow velocity and temperature measurements. Upon pulsed laser excitation, the tagged tracer molecules emit long-lived phosphorescence and become "glowing" markers that move with the working fluid. The phosphorescence emission of the tagged molecules is interrogated at two successive times after the same laser excitation pulse. The Lagrangian displacement of the tagged molecules over the prescribed time delay between the two interrogations is used to provide the estimate of the flow velocity. The simultaneous temperature measurement is achieved by taking advantage of the temperature dependence of phosphorescence lifetime, which is estimated from the intensity ratio of the tagged molecules in the two acquired phosphorescence images.

Three application examples are presented to demonstrate the feasibility and implementation of the molecular tagging techniques to study complicated and challenging thermal fluid problems. The first example is using the MTV&T technique to achieve simultaneous flow velocity and temperature field measurements in the wake of a heated cylinder to quantify the unsteady heat transfer process from the heated cylinder to the surrounding fluid flow in order to elucidate the underlying physics of the thermal effects on the wake instabilities behind the heated cylinder operating in mixed and forced heat convection regimes. The second example is related to applying the lifetime-based MTT technique to achieve simultaneous measurements of droplet size (in terms of volume, height, contact area, and the contact angle of the droplet) and temporally-and-spatially-resolved temper-

ature distributions within micro-sized, icing water droplets to quantify the unsteady heat transfer and phase changing process pertinent to aircraft icing phenomena. The third example considers the use of the MTV and MTT techniques to achieve simultaneous measurements of droplet size, velocity, and temperature of "in-flight" droplets to characterize the dynamic and thermodynamic behaviors of "in-flight" droplets in spray flows pertinent to the atomization and evaporation processes of the fuel droplets in combustion chambers of gas turbines and IC engines. These examples clearly demonstrate that the molecular tagging techniques (i.e., MTV, MTT and MTV&T) can serve as promising tools in the studies of various complex and challenging thermal fluid problems.

Acknowledgments The project is partially supported by the National Aeronautical and Space Administration (NASA) (Grant NNX12AC21A) with Mr. Mark Potapczuk as the technical officer. The support of the National Science Foundation (NSF) under award numbers of CBET-1064196, IIA-1064235 and CBET-1435590 is also gratefully acknowledged.

References

1. Adrian, R.J.: Twenty years of particle image velocimetry. Exp. Fluids **39**, 159–169 (2005)
2. Ainsworth, R.W., Thorpe, S.J., Manners, R.J.: A new approach to flow-field measurement—a view of Doppler global velocimetry techniques. Int. J. Heat Fluid Flow **18**, 116–130 (1997)
3. Komine, H., Brosnan, S.: Instantaneous, three-component, Doppler global velocimetry. In: Laser Anemometry—Advances and Applications 1991; Proceedings of the 4th International Conference, vol. 1 (A93–23776 08–35), pp. 273–277. (1991)
4. Elliott, G., Crafton, J., Baust, H.: Evaluation and optimization of a multi-component planar Doppler velocimetry system. 43rd AIAA Aerospace Sciences Meeting and Exhibit 10–13 January 2005, Reno, Nevada. p. AIAA 2005–0035 (2005)
5. Beutner, T., Elliott, G.: Forebody and leading edge vortex measurements using planar Doppler velocimetry. Meas. Sci. Technol. **12**, 378–394 (2001)
6. Zettner, C., Yoda, M.: Particle velocity field measurements in a near-wall flow using evanescent wave illumination. Exp. Fluids **34**, 115–121 (2003)
7. Jin, S., Huang, P., Park, J., et al.: Near-surface velocimetry using evanescent wave illumination. Exp. Fluids **37**, 825–833 (2004)
8. Devasenathipathy, S., Santiago, J.G., Takehara, K.: Particle tracking techniques for electrokinetic microchannel flows. Anal. Chem. **74**, 3704–3713 (2002)
9. Wang, D., Sigurdson, M., Meinhart, C.D.: Experimental analysis of particle and fluid motion in ac electrokinetics. Exp. Fluids **38**, 1–10 (2004)
10. Hu, H., Jin, Z., Nocera, D.: Experimental investigations of microscale flow and heat transfer phenomena by using molecular tagging techniques. Meas. Sci. Technol. **21**, 085401 (2010)
11. Hu, H., Jin, Z.: An icing physics study by using lifetime-based molecular tagging thermometry technique. Int. J. Multiph. Flow **36**, 672–681 (2010)
12. Hu, H., Koochesfahani, M.: A novel method for instantaneous, quantitative measurement of molecular mixing in gaseous flows. Exp. Fluids **33**, 202–209 (2002)
13. Hiller, B., Hanson, R.: Simultaneous planar measurements of velocity and pressure fields in gas flows using laser-induced fluorescence. Appl. Opt. **27**, 33–48 (1988)
14. Sakakibara, J., Adrian, R.J.: Whole field measurement of temperature in water using two-color laser induced fluorescence. Exp. Fluids **26**, 7–15 (1999)
15. Kim, H.J., Kihm, K.D., Allen, J.S.: Examination of ratiometric laser induced fluorescence thermometry for microscale spatial measurement resolution. Int. J. Heat Mass Transf. **46**, 3967–3974 (2003)
16. Coppeta, J., Rogers, C.: Dual emission laser induced fluorescence for direct planar scalar behavior measurements. Exp. Fluids **25**, 1–15 (1998)
17. Lavieille, P., Lemoine, F., Lavergne, G., et al.: Evaporating and combusting droplet temperature measurements using two-color laser-induced fluorescence. Exp. Fluids **31**, 45–55 (2001)
18. Thurber, M., Grisch, F., Hanson, R.: Temperature imaging with single-and dual-wavelength acetone planar laser-induced fluorescence. Opt. Lett. **22**, 251–253 (1997)
19. Hu, H., Koochesfahani, M., Lum, C.: Molecular tagging thermometry with adjustable temperature sensitivity. Exp. Fluids **40**, 753–763 (2006)
20. Omrane, A., Juhlin, G., Ossler, F., et al.: Temperature measurements of single droplets by use of laser-induced phosphorescence. Appl. Opt. **43**, 3523–3529 (2004)
21. Huang, D., Hu, H.: Molecular tagging thermometry for transient temperature mapping within a water droplet. Opt. Lett. **32**, 3534–3536 (2007)
22. Hu, H., Koochesfahani, M.M.: A novel technique for quantitative temperature mapping in liquid by measuring the lifetime of laser induced phosphorescence. J. Vis. **6**, 143–153 (2003)
23. Koochesfahani, M., Nocera, D.: Molecular Tagging Velocimetry. In: Handbook of Experimental Fluid Dynamics, pp. 362–381 (2007)
24. Gendrich, C., Koochesfahani, M.: A spatial correlation technique for estimating velocity fields using molecular tagging velocimetry (MTV). Exp. Fluids **22**, 67–77 (1996)
25. Stier, B., Koochesfahani, M.: Molecular tagging velocimetry (MTV) measurements in gas phase flows. Exp. Fluids **26**, 297–304 (1999)
26. Hu, H., Koochesfahani, M.: Molecular tagging velocimetry and thermometry and its application to the wake of a heated circular cylinder. Meas. Sci. Technol. **17**, 1269–1281 (2006)
27. Hu, H., Koochesfahani, M.: Thermal effects on the wake of a heated circular cylinder operating in mixed convection regime. J. Fluid Mech. **685**, 235–270 (2011)
28. Hiller, B., Booman, R.A., Hassa, C., et al.: Velocity visualization in gas flows using laser-induced phosphorescence of biacetyl. Rev. Sci. Instrum. **55**, 1964 (1984)
29. Lempert, W., Jiang, N., Sethuram, S., et al.: Molecular tagging velocimetry measurements in supersonic microjets. AIAA J. **40**, 1065–1070 (2002)
30. Lempert, W., Boehm, M., Jiang, N.: Comparison of molecular tagging velocimetry data and direct simulation Monte Carlo simulations in supersonic micro jet flows. Exp. Fluids **34**, 403–411 (2003)
31. Miles, R., Grinstead, J.: The RELIEF flow tagging technique and its application in engine testing facilities and for helium-air mixing studies. Meas. Sci. Technol. **11**, 1272–1281 (2000)
32. Miles, R., Zhou, D., Zhang, B., et al.: Fundamental turbulence measurements by RELIEF flow tagging. AIAA J. **31**, 447–452 (1993)
33. Ribarov, L., Wehrmeyer, J., Hu, S., et al.: Multiline hydroxyl tagging velocimetry measurements in reacting and nonreacting experimental flows. Exp. Fluids **37**, 65–74 (2004)
34. Pitz, R., Wehrmeyer, J.: Unseeded molecular flow tagging in cold and hot flows using ozone and hydroxyl tagging velocimetry. Meas. Sci. Technol. **11**, 1259–1271 (2000)

35. Orlemann, C., Schulz, C., Wolfrum, J.: NO-flow tagging by photodissociation of NO 2. A new approach for measuring small-scale flow structures. Chem. Phys. Lett. **307**, 15–20 (1999)
36. Krüger, S., Grünefeld, G.: Gas-phase velocity field measurements in dense sprays by laser-based flow tagging. Appl. Phys. B. **70**, 463–466 (2000)
37. Krüger, S., Grünefeld, G.: Stereoscopic flow-tagging velocimetry. Appl. Phys. B. **69**, 509–512 (1999)
38. Barker, P., Thomas, A.: Velocimetry and thermometry of supersonic flow around a cylindrical body. AIAA J. **36**, 1055–1060 (1998)
39. Rubinsztein-Dunlop, H., Littleton, B.: Ionic strontium fluorescence as a method for flow tagging velocimetry. Exp. Fluids **30**, 36–42 (2001)
40. Miles, R.B., Lempert, W.: Quantitative flow visualization in unseeded flows. Annu. Rev. Fluid Mech. **29**, 285–326 (1997)
41. Miller, S.: Photochemical reaction for the study of velocity patterns and profiles. BASc thesis, University of Toronto, Toronto (1962)
42. Popovich, A., Hummel, R.: A new method for non-disturbing turbulent flow measurements very close to a wall. Chem. Eng. Sci. **22**, 21–25 (1967)
43. Ojha, M., Hummel, R.: Development and evaluation of a high resolution photochromic dye method for pulsatile flow studies. J. Phys. E. **21**, 998–1004 (1988)
44. Falco, R., Gendrich, C., Chu, C.: Vorticity field measurements using Laser Induced Photochemical Anemometry (LIPA). In: Seventh Symposium on Turbulent Shear Flows (1989)
45. Falco, R., Nocera, D.: Quantitative multipoint measurements and visualization of dense solid-liquid flows using laser induced photochemical anemometry (LIPA). In: Rocco, M.C. (ed.) Particulate Two-Phase Flow, pp. 59–126, Chapter 3 (1993)
46. Lempert, W.R., Harris, S.R.: Flow tagging velocimetry using caged dye photo-activated fluorophores. Meas. Sci. Technol. **11**, 1251–1258 (2000)
47. Gendrich, C., Koochesfahani, M., Nocera, D.: Molecular tagging velocimetry and other novel applications of a new phosphorescent supramolecule. Exp. Fluids **23**, 361–372 (1997)
48. Hartmann, W., Gray, M., Ponce, A.: Substrate induced phosphorescence from cyclodextrin-lumophore host-guest complexes. Inorganica Chim. Acta **234**, 239–248 (1996)
49. Pouya, S., Van Rhijn, A., Dantus, M., et al.: Multi-photon molecular tagging velocimetry with femtosecond excitation (FemtoMTV). Exp. Fluids **55**, 1791 (2014)
50. Shafii, M.B., Lum, C.L., Koochesfahani, M.M.: In situ LIF temperature measurements in aqueous ammonium chloride solution during uni-directional solidification. Exp. Fluids **48**, 651–662 (2009)
51. Forkey, J., Lempert, W., Miles, R.: Accuracy limits for planar measurements of flow field velocity, temperature and pressure using filtered Rayleigh scattering. Exp. Fluids **24**, 151–162 (1998)
52. Forkey, J., Finkelstein, N., Lempert, W., et al.: Demonstration and characterization of filtered Rayleigh scattering for planar velocity measurements. AIAA J. **34**, 442–448 (1996)
53. Danehy, P., Byrne, S.O'., Houwing, A.P.: Flow-tagging velocimetry for hypersonic flows using fluorescence of nitric oxide. AIAA J. **41**, 263–271 (2003)
54. Clancy, P., Kim, J., Samimy, M.: Planar Doppler velocimetry in high speed flows. In: AIAA Fluid Dynamics Conference, AIAA 1996–1990 (1996)
55. Crafton, J., Carter, C., Elliott, G.: Three-component phase-averaged velocity measurements of an optically perturbed supersonic jet using multi-component planar Doppler velocimetry. Meas. Sci. **12**, 409–419 (2001)
56. Koochesfahani, M., Bohl, D.: Molecular tagging visualization and velocimetry of the flow at the trailing edge of an oscillating airfoil. In: 10th International Symposium on Flow Visualization (2002)
57. Hammer, P., Pouya, S., Naguib, A., Koochesfahani, M.: A multi-time-delay approach for correction of the inherent error in single-component molecular tagging velocimetry. Meas. Sci. Technol. **24**, 105302 (2013). (11pp)
58. Prasad, A.K., Adrian, R.J.: Stereoscopic particle image velocimetry applied to liquid flows. Exp. Fluids **15**, 49–60 (1993)
59. Hu, H., Saga, T., Kobayashi, T., et al.: A study on a lobed jet mixing flow by using stereoscopic particle image velocimetry technique. Phys. Fluids **13**, 3425 (2001)
60. Bohl, D., Koochesfahani, M., Olson, B.: Development of stereoscopic molecular tagging velocimetry. Exp. Fluids **30**, 302–308 (2001)
61. Pringsheim, P.: Fluorescence and Phosphorescence. Interscience, New York (1949)
62. Ossler, F., Aldén, M.: Measurements of picosecond laser induced fluorescence from gas phase 3-pentanone and acetone: implications to combustion diagnostics. Appl. Phys. B Lasers Opt. **64**, 493–502 (1997)
63. Ni, T., Melton, L.A.: Two-dimensional gas-phase temperature measurements using fluorescence lifetime imaging. Appl. Spectrosc. **50**, 1112–1116 (1996)
64. Lemoine, F., Antoine, Y., Wolff, M., et al.: Simultaneous temperature and 2D velocity measurements in a turbulent heated jet using combined laser-induced fluorescence and LDA. Exp. Fluids **26**, 315–323 (1999)
65. Sakakibara, J., Hishida, K., Maeda, M.: Vortex structure and heat transfer in the stagnation region of an impinging plane jet (simultaneous measurements of velocity and temperature fields by digital particle image velocimetry and laser-induced fluorescence). Int. J. Heat Mass Transf. **40**, 3163–3176 (1997)
66. Dabiri, D., Gharib, M.: Digital particle image thermometry: the method and implementation. Exp. Fluids **11**, 77–86 (1991)
67. Park, H.G., Dabiri, D., Gharib, M.: Digital particle image velocimetry/thermometry and application to the wake of a heated circular cylinder. Exp. Fluids **30**, 327–338 (2001)
68. Roshko, A.: On the development of turbulent wakes from vortex streets. Report 1191, National Advisory Committee for Aeronautics (1954)
69. Berger, E., Wille, R.: Periodic flow phenomena. Annu. Rev. Fluid Mech. **4**, 313–340 (1972)
70. Oertel Jr, H.: Wakes behind blunt bodies. Annu. Rev. Fluid Mech. **22**, 539–564 (1990)
71. Williamson, C.: Vortex dynamics in the cylinder wake. Annu. Rev. Fluid Mech. **28**, 477–539 (1996)
72. Zdravkovich, M.: Flow Around Circular Cylinders. Oxford University Press, Oxford (1997)
73. Incropera, F., Dewitt, D.: Introduction to Heat Transfer. John Wiley & Son, New York, NY (1996)
74. Politovich, M.K.: Aircraft Icing caused by large supercooled droplets. J. Appl. Meteorol. **28**, 856–868 (1989)
75. Bragg, M., Gregorek, G., Lee, J.: Airfoil aerodynamics in icing conditions. J. Aircr. **23**, 76–81 (1986)
76. Heinrich, A., Ross, R., Zumwalt, G., et al.: Aircraft icing handbook, vol. 2. Gates Learjet Corp Wichita KS (1991)
77. Gent, R., Dart, N., Cansdale, J.: Aircraft icing. Philos Trans R Soc Lond Ser A **358**, 2873–2911 (2000)
78. Bidwell, C.: Ice particle transport analysis with phase change for the E3 turbofan engine using LEWICE3D version 3.2. AIAA 2012–3037 (2012)
79. Bidwell, C.: Icing calculations for a 3D, high-lift wing configuration. AIAA 2005–1244 (2005)

80. Ryerson, C.C., Peck, L., Martel, C.J.: Army Aviation Operations in Icing Conditions. SAE Technical Paper. pp. SAE2003-01-2094 (2003)
81. Peck, L., Ryerson, C.C., Martel, C.J.: Army aircraft icing. Report no. ERDC/CRREL-TR-02-13, Cold regions research and engineering laboratory, engineering research and development center hanover NH (2002)
82. Jin, Z., Hu, H.: Icing process of small water droplets impinging onto a frozen cold plate. J. Thermophys. Heat Transf. **24**, 841–845 (2010)
83. Hu, H., Huang, D.: Simultaneous measurements of droplet size and transient temperature within surface water droplets. AIAA J. **47**, 813–820 (2009)
84. Castanet, G., Lavieille, P., Lemoine, F., et al.: Energetic budget on an evaporating monodisperse droplet stream using combined optical methods. Int. J. Heat Mass Transf. **45**, 5053–5067 (2002)
85. Li, H., Chen, F., Hu, H.: Simultaneous Measurements of Droplet Size, Velocity and Temperature of "In-flight" Droplets in a Spray Flow by using a Molecular Tagging Technique (AIAA). 2015 AIAA Science and Technology Forum and Exposition (SciTech2015). p. AIAA 2015–1224 (2015)
86. Ballew, R.M., Demas, J.N.: An error analysis of the rapid lifetime determination method for the evaluation of single exponential decays. Anal. Chem. **61**, 30–33 (1989)
87. Ke, J., Bohl, D.: Effect of experimental parameters and image noise on the error levels in simultaneous velocity and temperature measurements using molecular tagging velocimetry/thermometry (MTV/T). Exp. Fluids **50**, 465–478 (2010)